CORROSION PROTECTION OF CARBON STEEL BY ALUMINUM OXIDE NANO COATINGS USING SOLUTION PLASMA SPRAY TECHNIQUE

BY

Bander Faraj Al-Daajani

A Thesis Presented to the

DEANSHIP OF GRADUATE STUDIES

KING FAHD UNIVERSITY OF PETROLEUM & MINERALS

DHAHRAN, SAUDI ARABIA

In Partial Fulfillment of the
Requirements for the Degree of

MASTER OF SCIENCE

In

Chemical Engineering

May 2012

King Fahd University of Petroleum and Minerals, DHAHRAN
GRADUATE STUDIES

DEANSHIP OF GRADUATE STUDIES

The thesis, written by **BANDER FARAJ AL-DAAJANI** under the direction of his thesis advisor and approved by his thesis committee, has been presented to and accepted by the Dean of Graduate Studies, in partial fulfillment of the requirement for the degree of MASTER OF SCIENCE IN CHEMICAL ENGINEERING.

Thesis Committee

Dr. Usamah A. Al-Mubaiyedh
Department Chairman

Dr. M. S. Ba-Shammakh
Advisor

Dr. Salam A. Zummo
Dean of Graduate Studies

Dr. S. U. Rahman
Member

7/6/12
Date

Dr. M. M. Khaled
Member

DEDICATION

This thesis is dedicated to my family who provided me with all kind of support and help since the first day of my study. Also, this thesis is dedicated to my thesis advisor and all my friends who encouraged me and gave me all kind of inspiration and motivation to complete my study.

ACKNOWLEDGMENTS

First of all I thank Allah for helping me and giving me all kind of support to finish this study successfully.

I would like to acknowledge KFUPM / Chemical engineering department and all Faculty members for their support during my study for their kind support and help.

I wish also, to express my appreciation to Dr. Mohammad Ba-Shammakh who served as my major advisor. I also wish to thank the other members of my thesis committee Dr. Saleem U. Rahman and Dr. Mazen Khaled.

Also, I would like to thank Saudi Aramco for providing me with all kind of support such as provide the required equipment and materials that helped me to complete my MSc thesis study.

Table of Contents

List of Table

List of Figures

THESIS ABSTRACT

FULL NAME OF STUDENT	Bander Faraj Al-Daajani
TITLE OF STUDY	Corrosion Protection of Carbon Steel by Aluminum Oxide Nano Coatings Using Solution Plasma Spray Technique
MAJOR FIELD	Chemical Engineering
DATE OF DEGREE	May 2012

Metallic materials are widely used in the industry due to their superior mechanical properties and offshore structures are one example from the industry that usually uses the metallic materials such as carbon steel to support the daily operation of the concern oil and gas facilities. However, these metallic materials are subjected to corrosive conditions like aqueous environment. Therefore, a corrosion protection technique like external coating must be considered to prevent and mitigate corrosion process from initiation and then damage the target structures. Solution plasma spray technique (SPS) showed the ability to produce Aluminum oxide nano-structured coating by oxidizing aluminum nitrate nona-hydrate solution as achieved in this research.

Aluminum oxide nano-structured coating has several applications in the industry as a corrosion protection layer like insulator due to its high wear resistance and hardness. In this thesis, three different concentrations with three different flowrates of aluminum nitrate solution were involved to prepare different aluminum oxide nano-structured coating system. These coating systems were studied and characterized using several techniques such as AC Impedance, X-ray diffraction (XRD), Scanning electron microscope (SEM). Accordingly, the generated coating systems have

showed slight improvements. Furthermore, concentration of the aluminum nitrate nona-hydrate salt can be reduced by 40 – 50 wt. % and still can achieve same aluminum oxide structure.

ملخص الرسالة

الاسم: **بندر فرج الدعجاني**

عنوان الرسالة: **الحماية من التاكل للحديد الكربوني باستخدام طلاء اكسيد الألمنيوم المتناهي الصغر المطلي باستخدام تقنبة السائل المرشوش بالبلازما**

الختصص: **الهندسة الكيميائة**
تأريخ التخّرج: **مايو 2012**

تستخدم المواد المعدنية بشكل كبير في الصناعة نظرا لمواصفاتها الميكانيكية العالية والمنشأت البحرية تعتبر واحدة من الأمثلة من الصناعة التي تستخدم المواد المعدنية مثل الحديد الكربوني لتدعم عمليات التشغيل اليومية لمعامل الزيت والغاز. ومع ذلك هذه المواد المعدينة معرضه لعوامل التآكل مثل البيئة الملحية. وبالتالي فإن الحماية من التآكل مثل الطلاء الخارجي يجب أن يأخذ في الإعتبار ليمنع عليمة التآكل من البدء ومن ثم الإضرار بالمنشآت المعينة. تعتبر تقنية رش السائل بالبلازما لديها قدرة لإنتاج طلاء أكسيد الألمنيوم متنهاهي الصغر بواسطة إحراق محلوم نترات الألمنيوم كما أنجز في هذا البحث.

طلاء أكسيد الألمنيوم متناهي الصغر لديه عدة تطبيقات في الصناعة كـ طبقه حامية من التآكل مثل العوازل نظرا لمقاومته القوية للتعري ولصلابته. في هذا البحث ثلاثة تراكيز وثلاثة تدفقات مختلفة لمحلول نترات الألمنيوم شملت لتحضير نظام طلاء بأكسيد الألمنيوم المتناهي الصغر. و انظمة الطلاء هذه درست وحللت بإستخدام تقنيات مختلفة مثل جهاز التيار المتردد, والأشعة السينية, مجهر المسح الإلكتروني وبالتالي فإن انظمة الطلاء المنتجة اوضحة تحسناً بسيطاً. بالإضافة إلى ذلك فإن تركيز نترات الألمنيوم يمكن أن تقلل من 40% إلى 50 % وتعطي نفس التركيب من طلاء أكسيد الألمنيوم.

CHAPTER 1

1 INTRODUCTION

Metallic materials are widely used in the industry and in many other applications in our daily life. They are widely used in many industry applications such as oil and gas plants, power plants, aerospace, automotive industry, etc. Steel in general and carbon steel in particular are the most commonly utilized as metallic material in open-air structures and is used to make a wide range of equipment and metallic structures due to its low cost and good mechanical properties. Much of the steel that is manufactured is exposed to outdoor conditions, often in highly polluted atmospheres such as offshore where corrosion is much more severe than in clean non corrosive environments structures. The atmospheric corrosion of carbon steel is an extensive topic that has been studied by many researchers due to its wide applications and importance [1]. However, corrosion is a common problem in the material science and costs countries billions of money every year in order to mitigate and control the corrosion [2].

Therefore, great research efforts have been devoted over the years into the improvement of the corrosion resistance of different types of steel such as stainless steel, carbon steel, galvanized steel, etc. Different approaches have been proposed to extend the service life of steel constructions [3]. Hence, the metallic materials need to be protected against corrosion by providing a layer that face the aggressive environments and therefore, protect the target materials. This technique is called

coating which is one of the most common methods that are being used to protect the materials from corrosion since it is simple to apply and fast.

There are two main types of coatings can be widely utilized as a method of protection, metallic and non-metallic coatings. Non-metallic coating can be classified into two main categories, organic and inorganic coating such as ceramic coating like aluminum oxide coating. The metallic coating is one option that came into the picture since decades. The meaning of metallic coating is as simple as applying metal which has better mechanical properties and corrosion resistance on top of the target metals which has poor mechanical properties and corrosion resistance. Metallic coatings have been proved to reduce the rate of corrosion of steel in various environments while scientists and engineers have been developing novel metallic coatings in a purpose to prevent steel from corroding [4, 5]. This metallic coating can be applied by using thermal spray technology which is a widely used technique for producing metal, ceramic or mixed metal-ceramic coatings on metal substrates.

Therefore, ceramic coating such as (Al_2O_3) is the main subject in this research and will be produced by a thermal spray technique. There are two types of thermal spraying are plasma and flame spraying, both of which are based on the projection of molten or semi-molten particles onto a prepared substrate [6]. Thermal spraying is the generic name for a family of coating processes in which a coating material is heated rapidly in hot gaseous medium and simultaneously projected at a high velocity onto a prepared substrate where it builds up to produce the desired coating. Thermal Spray Coating (TSC) is basically a process of spraying molten materials into metallic surface where solidified molten sprayed material builds up to provide a coating layer.

The main objective of applying such coating is to enhance its resistivity to wear, heat, and corrosion.

Like any other process, thermal spray processes rely upon a set of inputs to produce desired outputs. A performance evaluation of thermal spray processes can be conducted by determining how effectively the process utilizes the inputs to produce the outputs. For different thermal spray processes of arc wire, combustion wire, plasma, etc. the inputs can be defined as sources of energy in terms of electrical power, the energy stored in combustible gases, and the potential energy stored in compressed gases. Each of these inputs can also be associated with a cost per unit amount. The outputs of a thermal spray process that is utilized is the energy contained in the particles that result in the formation of a coating. The spray material has to be endowed with a certain amount of thermal and kinetic energy to form the coating. Thus it is possible to evaluate each process in a comparative way and rate the processes in terms of overall performance [7].

In this study, the plasma spray technique is utilized to apply ceramic coatings on carbon steel substrate. The bond coat was applied first on top of the substrate and it was cobalt chromium aluminum yttrium alloy (CoCrAlY). Such bond coat is usually employed in TBCs to improve their structural effectiveness and the adhesion between the ceramic based top coat and the superalloy substrate. In addition, the bond coat plays an important role in protecting the substrate from oxidation, having the thickness of 75–150 μm. CoCrAlY alloy has been widely used as metallic protective coatings or the bond coats in thermal barrier coatings (TBCs) to protect the underlying superalloy from oxidation and hot-corrosion. CoCrAlY coating layer

exhibits excellent oxidation and hot corrosion resistance due to its high level of Al and Cr content [8, 9].

On the other hand, the Solution Plasma Spray feeder (SPS) was utilized to inject the raw material which is aluminum nitrate as liquid into the flame of the plasma gun. The Solution Plasma Spray (SPS) system uses standard plasma guns and robotics, but the conventional powder feeding system is replaced by a solution precursor storage, feeding and injection system [10]. Hence SPS is an attachment that can be integrated to plasma spray system and inject the desired solution directly into the generated flame. It is a new approach and just recently introduced to the industry. In general SPS is appended to an existing spray facility to further enhance efficient application of protective nano-coatings. The main principle is based on using liquid spray media instead of the common powder form. It is for delivery and injection of liquid precursors, specifically used in the solution plasma spray (SPS). It is designed to deliver the liquid solution from multiple containers to a liquid injector, preferably an atomizing-type nozzle. This system was used to produce Aluminum oxide nano-structured coating which is the main subject of this study.

The metallic nano-structured coatings play important roles by providing a protective layer on the desired equipment or other metallic materials. This protective layer provides the required protection against corrosion and therefore, extends the service life of the materials. It is well known that engineering quality Al_2O_3 ceramic coating shows excellent properties of chemical stability and corrosion resistance. The sprayed ceramic coating layer by plasma spray system can change the corrosion behavior of the metal in a corrosive solution and shows an outstanding protection against

corrosion. Also, it shows excellent behavior against wear and corrosion. Therefore, due to its high hot hardness, chemical durability and oxidation resistant properties, there has been an enormous interest in the development of crystalline alumina films for their application as wear resistant protective coatings on high-speed machine tools for milling and cutting of cast iron and low carbon steel and as an insulating material in the industry. It can be produced in several transient, metastable structures like γ-, η-, θ-, δ- and κ-phases but the most stable one is α-phase [11, 12].

Based on the above information, the coating system which is produced in this MSc thesis work consists of bond coat (CoCrAlY) and top coat which is Al_2O_3 applied on prepared carbon steel substrate.

OBJECTIVE

The main objective of this MSc thesis work is to produce aluminum oxide coating by using an innovative technique which is solution plasma spray system. This system can be considered as one technique that can produce aluminum oxide coating beside the conventional techniques such as Physical Vapor Deposition (PVD), Chemical Vapor Deposition (CVD) and so on. Another reason is to study the effect of aluminum nitrate concentration and flowrate on the structure and effectiveness of the coating system. Three different concentrations and flowrates of Aluminum nitrate solution were investigated in this research work in the experimental work chapter 3.

In addition, characterization by using different innovative techniques such as Scannin Electron Microscope (SEM) and X-ray Diffraction (XRD) were utilized in this research to study the effect of both (solution concentration and flowrate) on the structure of the aluminum oxide coating and adhesion promotion.

The main purpose of trying different concentrations and flowrate was to come up with best coating parameters by optimizing the concentration and flowrate of the aluminum nitrate solution. This will help in reducing the cost of used raw material by decreasing aluminum nitrate content and decrease solution consumption by reducing solution flowrate during the spray process.

The literature review pertaining in this study is presented in chapter 2 while chapter 3 describes the experimental procedure and apparatus. Results and discussion section is presented in chapter 4 and finally chapter 5 contains the conclusion of the work and summarized the recommendations for future work.

CHAPTER 2

2 LITERATURE REVIEW

Most of the industry applications are made from metallic materials such as oil and gas plants, refineries, power plants automotive industry, aerospace and so on. Therefore, Metallic materials are considered to be one of the most important constituents in our daily life. Accordingly, any source of risk leading to a degradation of such materials will directly threat our infra structures and economy. Corrosion of metallic materials is a natural phenomenon leading to a serious degradation in metallic materials.

in general corrosion is a deterioration of metallic materials due to an electrochemical reaction between a metal and the surrounding environment [13-15]. Iron and its alloys are the most common metals used by many applications in the industry and our daily life and to fully understand the electrochemical nature of corrosion, it must be realized that corrosion is a process that involves a transfer of electric charges resulting in a metal extraction from its minerals. This principle can be easily explained by considering an example of carbon steel placed in seawater. This carbon steel sample will be exposed to two obvious reactions as follow:

1) Anodic reaction: this is an oxidation reaction which iron valence increases from 0 to +2 and librating electrons. The anodic site is the place where the metal 'dissolves' according to the following oxidation reaction:

$$Fe \rightarrow Fe^{2+} + 2e^{-} \quad (1)$$

2) cathodic reaction: for the anodic reaction to take place there must be a cathodic process where the produced electrons can be consumed. This cathodic process occurs on what is known as cathodic sites where a reduction reaction of oxygen takes place according to the following reaction:

$$O_2 + 2H_2O + 4e^- \rightarrow 4OH^- \quad (2)$$

Based on the above argument, the electrons produced by the anodic reaction are consumed by the reduction reaction of oxygen. This scenario is most likely to happen in the case of steel in seawater. On the other hand, there are other cathodic reactions, as it is shown below, that could happen depending on the nature of the environment:

$$O_2 + 4H^+ + 4e^- \rightarrow 2H_2O \quad (3)$$

$$2H^+ + 2e^- \rightarrow H_2 \quad (4)$$

$$2H_2O + 2e^- \rightarrow H_2 + 2OH^- \quad (5)$$

Hence, there are four main components for the corrosion to take place and they are:

1) Anodic sites where the oxidation reaction takes place.
2) Cathodic sites where the reduction reaction takes place.
3) Electrolyte where the ionic current is happily flowing. It is usually the environment that is in contact with the structure.
4) Connection between the anode and the cathode. It is the path where the electrons are moving. In most cases, it is the structure itself.

In general, the corrosion process (anodic reaction) of the metal dissolving as ions generates some electrons that are consumed by a secondary process (cathodic reaction). These two processes have to balance their charges. The sites hosting these two processes can be located close to each other on the metal's surface, or far apart depending on the materials. This simple observation has a major impact on many aspects of corrosion prevention and control for designing new corrosion monitoring techniques to avoid the most insidious or localized forms of corrosion [13–16]. As it was mentioned earlier, the presences of the anodic and cathodic sites are very essential for corrosion to take place. For these sites to exist there must a potential difference on the surface of the metal. There are many causes for such difference; one important mechanism is oxygen concentration cell corrosion, in which the oxygen concentration in the electrolyte varies from place to place. The part where more oxygen is available will be the cathodic site where the other part is going be the anodic site and will suffer corrosion [17]. Such difference in potential can also be initiated in the case of coupling two different metals. At this case, the corrosion rate will increase on one metal while a reduction in the corrosion rate will be noticeable on the other (Galvanic Corrosion) [18].

There are various forms of corrosion that can take place depending on the environment and the design of the equipment that suffers corrosion. The corrosion types observed can be summarized as the followings [15]:

- General corrosion
- Uniform Corrosion.
- Galvanic Corrosion.
- Crevice Corrosion.

- Pitting Corrosion.
- Environmental Induced Cracking.
- Hydrogen Damage.
- Intergranular Corrosion.
- Erosion Corrosion.

All of these forms are already discussed in more details in literature and it is out of the scope of this master thesis.

Corrosion is a natural phenomenon which is difficult to be eliminated but it can be reduced or mitigated. However, if the rate of corrosion can be reduced so that the amount of corrosion which occurs over the lifetime of structure is negligible, corrosion has been considered, for all practical purposes, to be eliminated. Basically, this mission mainly depends on the idea of reducing the corrosion current.

Therefore, thermodynamics and the kinetics of corrosion are very essential to design the appropriate protection method. One obvious solution to reduce the corrosion rate that might happen in a given application is to choose noble materials that resist the corrosive environment that could present in the application of interest. Unfortunately, this way to solve the problem is sometimes very costly and usually corrosion engineers do not consider this option in many applications. Therefore, considering the electrochemical principles and the nature of the corrosion process taking place in the interested application is the path to follow in order to design the right method.

Based on the above discussion, there are three main corrosion protection methods that are commonly used and they are cathodic protection, corrosion inhibitors and coatings. These methods can be summarized as follows:

1) Cathodic Protection (CP): the basic principle of (CP) is not complicated. A metal dissolution is reduced through the application of a cathodic current. Cathodic protection is often applied to coated structures, with the coating providing the primary form of corrosion protection. The CP current requirements tend to be excessive for uncoated systems. Cathodic protection has probably become the most widely used method for preventing the corrosion. Cathodic protection basically reduces the corrosion rate of a metallic structure by reducing its corrosion potential, bringing the metal closer to an immune state. The two main methods used in any CP system can be summarized as it follows:

- Using sacrificial anodes with a corrosion potential lower than the metal to be protected.
- Using an impressed current provided by an external current source

2) Corrosion Inhibitors: They are chemical compounds added to the corroded system to form a layer on the surface. This layer is formed due to a reaction between these chemicals and the corroded surface. Inhibitors can be widely used in many applications such as acidic environment, cooling water systems and production of crude oil. For neutral solution, depending on the mechanism that an inhibitor follows to protect a metal, corrosion inhibitors can be classified into three main categories: cathodic, anodic and mixed inhibitors [19]. For example, the presence of zinc-polyphosphate solution in 3.5% NaCl will inhibit the mild steel by forming a 3D layer on the surface. Such layer will act as a barrier to hinder the diffusion of oxygen to the surface. In this case, the cathodic reaction on the surface of the metal will be disturbed and a decrease in the corrosion rate will be detected. Such inhibitor can be considered to be a cathodic inhibitor since its protection mechanism is mainly affecting the

cathodic process [20]. For anodic inhibitor, the presence of some chemical such as nitrite anions in neutral solution will form a layer blocking the anodic sites. As a result of this blocking the rate of metal dissolution will be reduced leading to reducing the corrosion rate. Some other inhibitor such as chromate which can affect both the anodic and the cathodic processes and can be classified as a mixed inhibitor [15].

For acidic environment, the cathodic process is mainly hydrogen evolution by reducing H+ present to hydrogen gas. The inhibition mechanism in such environments involves blockage of the metal surface by the inhibitor molecules that are adsorbed on the surface. In general, the adsorption process is highly affected by the nature of the metal surface and the chemical structure of the inhibitor. The presence of amino acid in 1.0 M HCl solution will follow the mentioned mechanism to inhibit some metals such mild steel [21].

3) Coatings: Two main types of coating can be widely used, metallic and non-metallic coatings. Both types have different approach and mechanisms to provide the required protection. This corrosion protection is the heart of this master thesis and only the non-metallic coating (ceramic coating) will be discussed and researched in this thesis. The properties of the coating itself are very critical in determining how good is the coating. Also, non metallic coating can be classified into two main categories: organic and inorganic coatings. In this thesis, inorganic coating which is aluminum oxide coating will be discussed in more details.

Al_2O_3 coating has high wear resistant due to its highly plasma erosion resistant characteristics is an interesting coating material, especially for use as a wear resistant layer [22]. It is a very important ceramic which is tremendously used at high temperature applications and used as corrosion resistant refractory material. This is

due to its high hardness, chemical durability and oxidation resistant properties. Aluminum oxide coating thin films are also of interest in microelectronics industry as an insulator due to their excellent electrical properties and high dielectric constant. Aluminum oxide coating is known to exist in several transient, metastable structures like γ-, η-, θ-, δ- and κ-phases but the most thermodynamically stable is α-phase [12]

This kind of ceramic coating can be produced by using several methods such as Physical Vapor Deposition (PVD), Chemical Vapor Deposition (CVD), Sputtering and Solution Plasma Spray System (SPS) which is the method that has been used in this work to produce aluminum oxide coatings. However, PVD and CVD techniques have some disadvantages like void formation in the coating in case of PVD or surface roughness problem in case of CVD and the research is still going on to overcome these problems [12,23]. In the other hand, Atmosphere plasma spraying (APS) is a commonly used method for preparing aluminum oxide coatings. However, in traditional APS the powders are injected into the plasma flame outside of the nozzle, or powders are injected into the inside of the nozzle through a hole in the radius direction of the nozzle side. Also, the porosity of Al_2O_3 coatings deposited by APS is usually 5–10% which refers to the type of plasma spray torch [24].

Nowadays intensive researches are conducted on the elaboration of layers structured at the nano scale to reach better properties. It is possible to produce finely structured layers and suspension plasma spraying (SPS) can be easily implemented on current plasma spray system. Indeed, SPS is a recent process and an alternative to APS which allows producing finely structured and thinner layers due to the smaller size of the feedstock particles, ranging from a few tens of nanometers to a few micrometers, injected into plasma as a liquid precursor. However, the set of parameters controlling

the final coating architecture and properties are not yet fully mastered. Moreover, the functional properties of SPS layers are not intensively studied [25].

Therefore, SPS will be discussed in more details in the following section. The following section will shed the light on the plasma spray system which was used in this MSc study as a source of high temperature and then will focus on the SPS as a source of the feeder solution.

2.1 Solution Plasma Spray System

Plasma spray is one technique that can be used to apply coatings at high temperature. It is a well established and versatile technique to produce coatings for improving wear, thermal and corrosion resistance. The plasma has the highest temperature (typically: 6000-15000 ^{o}C) among all the thermal spray processes. As a result, plasma spraying technology can deposit high melting point material such as ceramics. Taking into consideration fast deposition rate, possibility of large area sample as well as low cost, plasma spraying process is the most commonly used to deposit various kinds of coatings in industry nowadays [26].

Simply, plasma gas which contains argon, hydrogen, helium and nitrogen flows around the cathode and through the anode which is shaped as a narrow nozzle and plasma is initiated by a high voltage discharge which causes ionization. The resistance heating from the arc causes the gas to reach extreme temperature dissociate and ionize to form plasma. The plasma discharges from the anode nozzle as a free or neutral plasma flame. Material in the form of powder is injected into a very high temperature plasma flame, where it is rapidly heated and accelerated to a high velocity. The hot material impacts on the substrate surface and rapidly cools forming a coating. This plasma spray process carried out correctly is called a "cold process". The powder particles of the desired coating material are fed axially into a hot gas stream then into

a spray gun to be melted and propelled to the surface of the samples to be coated. The gun consists of three sections: a mixing zone, combustion zone and the nozzle as illustrated in Figure 2-1

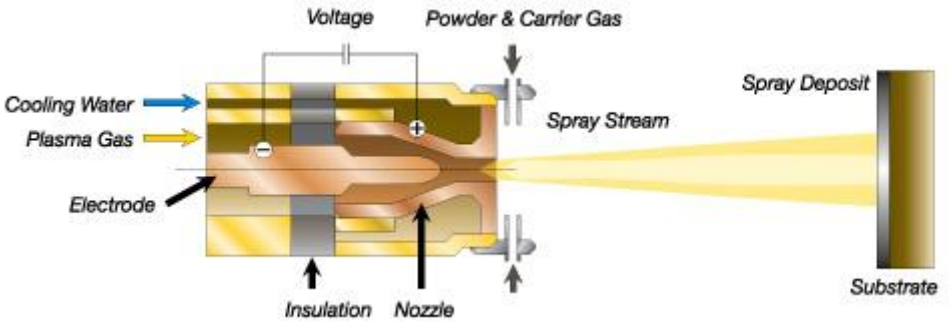

Figure 2-1 Schematic representation of Plasma Spray Gun [27].

Instead of using the conventional powder feeder, the SPS was utilized to produce nanostructured coatings. The SPS is newly introduced system that can produce aluminum oxide coating. It has been developed to produce nano-structured coating by using aluminum nitrate solution. The proposed SPS system is an attachment that can be integrated to plasma spray system and inject the desired solution directly on the generated flame. It is a new approach and just recently introduced to the industry. This SPS is appended to an existing spray facility to further enhance efficient application of protective nano-coatings. The system consists of three main components which are control unit, storage tanks and three hoses. The main principle is based on using liquid spray media instead of the common powder form. It is for delivery and injection of liquid precursors, specifically used in the solution plasma spray (SPS). It is designed to deliver the liquid solution from multiple containers to a liquid injector, preferably an atomizing-type nozzle as illustrated in figure 2-2 [28].

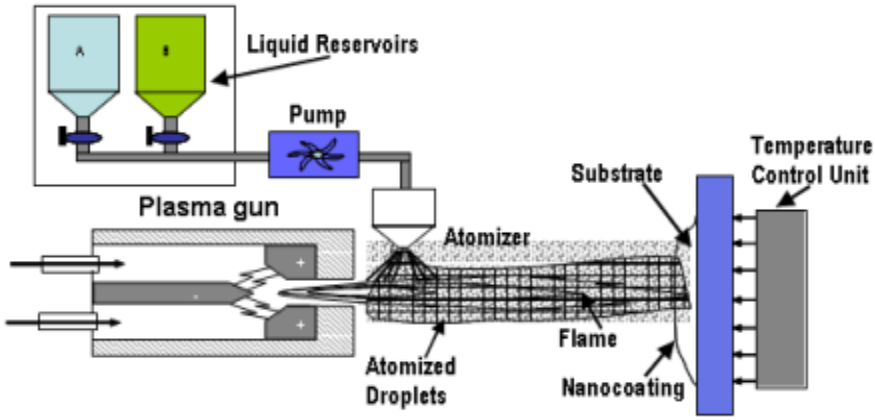

Figure 2-2 demonstrates the main components of Solution Plasma Spray system [28]

But in order to achieve good coating, the surface preparation should be considered to provide good adhesion between the substrate and the coating layer. Hence there are two forces holding the coating to the metals surface, which are mechanical and chemical forces.

- Chemical Forces: When a coating is applied to a surface, there is a coating/metal interaction that is taking place. It should bear in mind that this interaction is not between the coatings and metal itself but it is between the coating and the oxide layer present. Therefore, the adhesion is promoted by forming hydrogen bonds between the groups on the resin molecules and the oxide on the surface [29].
- Mechanical Forces: This type of forces or attraction is highly affected by the surface profile (roughness). Figure 2-3 shows three different mechanisms of the mechanical forces to hold the coating to the metal surface.

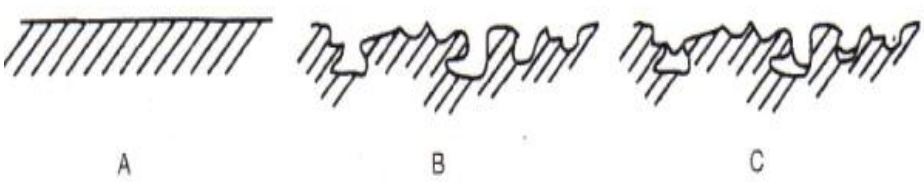

Figure 2-3: The Effect of the Surface Profile [29]

As mentioned before, the surface of the substrate can be classified into three categories as it is shown in figure 2-3. If the coating was applied on a smooth surface such as figure (2-3 A), the only force holding the coating is the interfacial attractive force between the coating and the surface. On the other hand, considering the surface in figure (2-3.B), the roughness of the surface will play a major role in the adhesion strength. In the case of applying a coating on such surface, two factors will affect the adhesion strength. As it is shown, in some places, there are undercuts in the substrate. To pull the coating off the substrate, one would either have to break the substrate or break the coating to separate them. Another factor is that the actual contact area between the coating and the substrate is significantly larger than the one in the case of smooth surface. Therefore, a rough surface is better to obtain good adhesion. On the other hand, the surface roughness can be a disadvantage some times, if the coating penetration is not effective especially in cases such as the one shown in figure (2-3 C). In this case, the coating cannot penetrate and reach some places and the effect of the surface roughness is not going to be great and the contact areas will be smaller than it is aimed to be. Furthermore, when water penetrates through this coating, it can reach areas where there is no coating present. Consequently, corrosion can take place under the coating [29]. This step can be achieved by using grit blast machine with 300 micron aluminum oxide grit or lower size.

After achieving the necessary roughness on the prepared substrate then the coating can be applied using SPS system to provide the protective coating layer. Following that the produced samples can be tested under different environment like aqueous solution in case of this thesis study with utilization of Electrochemical Impedance method to evaluate the corrosion activity under the coating layer. Also, the samples

can be characterized by using environmental scanning electron microscopy (ESEM) and X-ray diffractometry (XRD).

The following section will focus mainly on the characterization and testing methods that were conducted in this thesis.

2.2 Electrochemical Impedance Spectroscopy (EIS)

Electrochemical impedance spectroscopy (EIS) has been used widely for monitoring the rate if corrosion process in conducing media. This technique is usually used to predict the polarization resistance, Rp, in order to calculate the corrosion rate using Stern-Geary relationship:

$$i_{corr} = ß_a ß_c /(2.303 R_p (ß_a + ß_c)) \quad (6)$$

Where, ßa and ßc are the Tafel coefficient for the anodic and the cathodic reactions respectively [30, 31]. It is not a simple technique and understanding its mathematical background is essential to analyze the data obtained from such technique. For this reason, the following section will briefly introduce the mathematical principles used to generate the EIS data.

2.2.1 Theory of (EIS)

For any scientist to understand this technique, the basic electrical background must be understood. EIS is mainly based on electrochemistry and the data obtained can be transformed to an equivalent electric circuit. The components in this equivalent electric circuit can be interpreted to describe the corrosion process taking place on the metal of interest. For any corroding metal, the simplest equivalent circuit can take the following form:

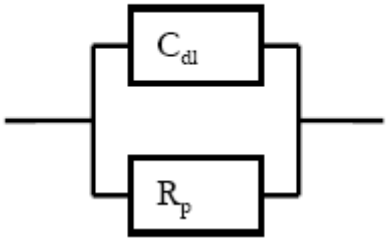

Figure 2-4: Simple Equivalent Circuit for a Corroding Metal [32].

In the figure 2-4, R_p represents the polarization resistance and C_{dl} represents the double layer capacitance. The main principle for EIS is based on applying an AC voltage and then measuring the resulting AC current [32, 33]. It is also important in this technique to consider the fact that both voltage and current are the time dependent. If a voltage applied to the above circuit, based on Ohm's Law, the current passing through the resistance can be expressed as follows:

$$I_R(t) = \frac{V(t)}{R_p} \tag{7}$$

This current is usually current is known as the Faradaic current as it is related to oxidation or reduction of species. In this case, the amount of materials oxidized or reduced can be related to the current by Faraday's Law [32]. As a result of the applied voltage, the current passing through the capacitance can be calculated by the following relationship. It must be noticed that the current through the capacitance depends on the rate of the change of the voltage and not on the voltage itself [31, 32]:

$$I_c(t) = C_{dl}\frac{dV(t)}{dt} \tag{8}$$

By using equations (7) and (8), the total current passing through the equivalent circuit can be calculated as:

$$I(t) = \frac{V(t)}{R_p} + C_{dl}\frac{dV(t)}{dt} \tag{9}$$

The above mathematical approach is the simplified principle of EIS. It is well known that the AC signals generated by EIS are sinusoidal signals and consequently the above approach must be modified. Accordingly, the voltage applied can be presented as:

$$V(t) = V_0 \sin(\omega t) \tag{10}$$

Hence, equation 10 can be plotted as:

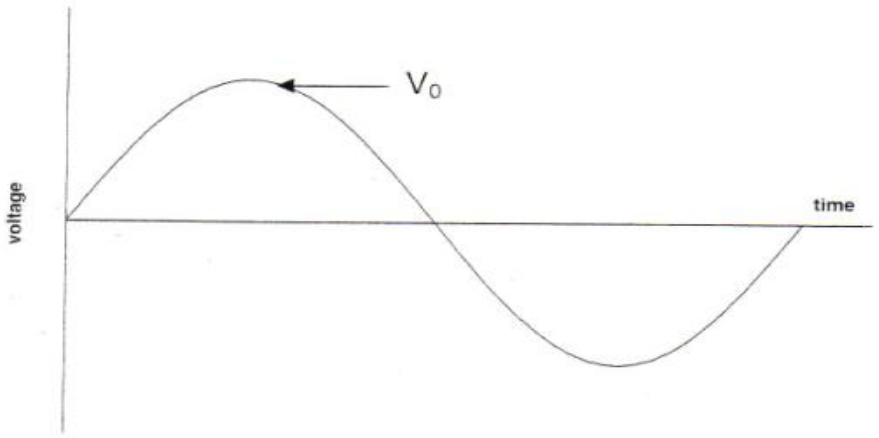

Figure 2-5: Sinusoidal Voltage Signal [32]

Where, V_0 is the peak (maximum) amplitude of the voltage and ω is the angular frequency of the sine wave and having the unit of (radians / second). It can be presented as it follows [32]:

$$\omega = 2\pi f, \text{ (f is the frequency in Hz)} \tag{11}$$

Consequently, the rate of change of the sinusoidal voltage in can be calculated as:

$$\frac{dV(t)}{dt} = V_0 \omega \cos(\omega t) \tag{12}$$

Therefore, the total current passing through the equivalent circuit can be obtained by the following equation:

$$I(t) = \frac{V_0}{R_p} \sin(\omega t) + V_0 \omega C_{dl} \cos(\omega t) \tag{13}$$

There are two ways of presenting the data and based on that two main plots can be generated from the impedance instrument. The following sections will give a brief introduction describing these two plots.

- Nyquist plot

This plot is one way of presenting the impedance data obtained for a corroding sample. It is basically a plot of the imaginary part of the impedance against the real part [32]. Figure 6 shows an example of a Nyquist plot for a corroding sample:

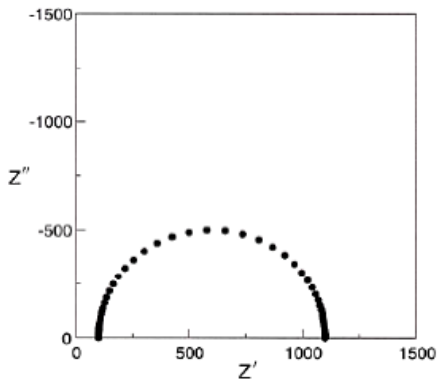

Figure 2-6: Nyquist Plot for Corroding Sample [32]

In the above figure, each point shows the impedance value at a specific frequency. The solution resistance R_s is obtainable from the high frequency intercept with the real axis, and the total resistance $R_s + R_p$ can be obtained from the low frequency intercept. At the maximum point at the semi-circle the frequency can be calculated as:

$$\omega_{\max} = 2\pi f_{\max} = \frac{1}{R_p C_{dl}} \tag{14}$$

By having such plot, the values of the components in the equivalent circuit can be calculated and then can be interpreted to physical meanings describing the corrosion process that takes place [32].

- Bode Plots

These plots represent a different way to present the impedance data. In this section, examples of Bode plots will be shown as it follows:

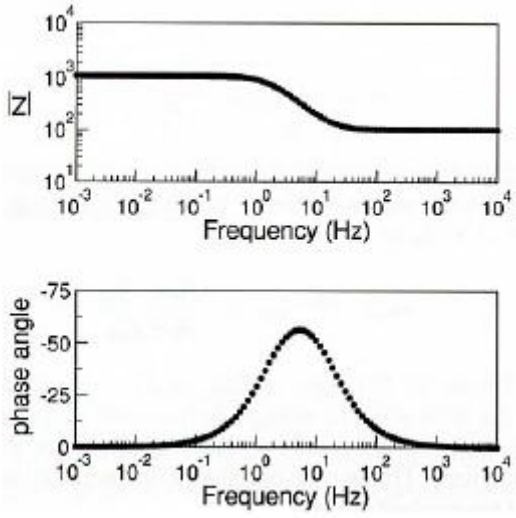

Figure 2-7: Bode Plots for the Equivalent Circuit of a Corroding Sample [32]

The above discussion about EIS is the basic foundation that will be used to understand and evaluate the aluminum oxide coating. EIS has many applications and many research areas are using such technique to understand many systems. In this MSc thesis, EIS was used mainly to study the behavior of carbon steel samples coated with aluminum oxide nanocoating. Figure (2-4) shows the simplest equivalent circuit that represents a corroding sample. In the case of coated metal sample immersed in the

electrolyte, the circuit in figure (2-4) cannot be longer used as an equivalent circuit while another model has been proposed. According to Mansfeld, for a coated sample and immersed in an electrolyte, the following equivalent circuit will represent such system:

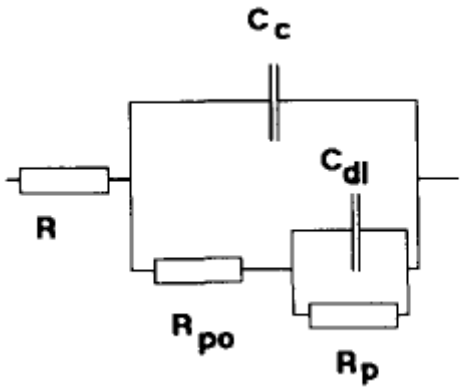

Figure 2-8: Equivalent Circuit for Coated Sample [34]

As it is shown, the impedance instrument will look at the system as an electric circuit while the scientists have to interpret such circuit to a physical meaning that can serve their targets. There are five components forming the above circuit:

- Solution Resistance: It appears in the circuit as R which is the resistance between the sample and the counter electrode (if three electrodes system is used).
- Pore or coating resistance (R_{po}): This is a property describing the coating itself. It is a measure of the corrosion protection ability of the coating. The value of this resistance is expected to decrease with time due to the stresses building up inside the coating as a result of the corrosion products formation under the coating [34 – 39].
- Coating Capacitance (C_c): It is also related to the coating itself and it is an indication of the water uptake inside the coating. The value of such parameter is expected to increase with time due to water penetration inside the coating. The coating capacitance can be presented by the following formula:

$$C_{coat} = \frac{\varepsilon_o \varepsilon A}{d} \qquad (15)$$

Where,

ε is the dielectric constant of the coating, and

A is the surface area of coating and d is the thickness of the coating [35, 40].

- Polarization resistance (R_p): It is sometimes called charge transfer resistance, R_{ct}, which is an indication of the electrochemical reaction occurring at the metal interface [34 – 36, 41, 42].
- Double Layer Capacitance (C_{dl}): It is also an indication of the electrochemical reaction that might occur under the coating [34, 35, 42, 43].

  Based on the above discussion, running an electrochemical impedance spectroscopy experiment on a coated sample can provide information describing both the coating and the corrosion process occurring under the coating.

2.2.2 X-Ray Diffraction (XRD)

This technique has many applications and can provide some critical information that can contribute significantly to understand the structure of the treated nanomaterials and the coatings prepared. X-rays were discovered in 1895 by a German physicist called Roentgen who could not fully understand the nature of these rays that were unknown at that time. These rays are invisible, travel in straight lines and they have a penetrating behavior enable them to easily pass the human body. In 1912, the nature of these rays was fully understood and the phenomenon of x-ray diffraction by crystals was discovered at that time and was used to investigate the fine structure of some materials [44, 45]. These rays are electromagnetic radiations of the same nature as light but with shorter wavelength ranging from 0.5 to 2.5 Angstrom (A) whereas it is 6000 A for light. X-rays travel in space as sinusoidal waves and it can be considered as a stream of particles called photons. Each photon is carrying an amount of energy that can be calculated as:

$$E_{photon} = 6.62 \times 10^{-27} \times f \qquad (16)$$

Where **f** is the frequency of the waves and can be related to the wavelength based on the following equation:

$$\text{Wavelength} = 3.00 \times 10^{10}\,(\text{cm/sec})/f \qquad (17)$$

This stream of photons is travelling as a wave that is carrying energy. The rate of the flow of this energy through a unit area perpendicular to the direction of the wave is called intensity. When such rays are encountered by any form of matter, part of these rays is absorbed and the other part is transmitted. A matter can absorb x-rays in two ways, by scattering and by true absorption. [45].

When such rays are encountered by any form of matter, part of these rays is absorbed and the other part is transmitted. A matter can absorb x-rays in two ways, by scattering and by true absorption. The scattering process of x-rays by the atoms in any matter is similar to the scattering of the visible light by any object, such as dust particles in air. The true absorption can be explained by quantum physics which is not related to this MSc thesis and will not be covered in this study [45].

Therefore, the scattering process can be used to study the structure of any crystalline materials as it will be shown later. Before discussing this issue, it will be useful to know the way these rays are produced before using them in any study. Such rays can be generated if high speed electrons collide with a metal target [45, 46]. Consequently, any x-ray tube should contain:

- A source of electrons.
- A high accelerating voltage.
- A metal target.

Generating such rays has contributed significantly to science by being used in many applications such as X-Ray Diffraction technique (XRD). Hence, it is useful to introduce the main principle used to utilize XRD.

It is a very important technique that is mainly used to investigate any crystalline materials. It is mainly using the principles of x-ray and its properties in diffraction to produce some information about some materials. In such technique the x-rays are generated by the same approach mentioned above. It contains an x-ray tube having two main electrodes, anode and cathode. The anode is usually the metal target such as copper which is maintained at ground potential. The cathode is the electron source and it is usually a tungsten filament which is maintained at high negative potential, normally 30000 to 50000 volts. The presence of such high potential between the two

electrodes will help to accelerate the electrons beam in the tube. The cathode is heated by using a filament current with a value of 3 amps to emit electrons that are rapidly drawn by the high voltage to hit the metal target.

As a result of such process and based on quantum physics, the anode will generate some kind of radiation which is known as x-rays. After generating these rays, they escape from the tube through some windows in the tube housing. After that, the x-rays are detected by using a fluorescent screen, photographic film and ionization device which is used to measure the intensity of the rays, a detailed description can be found in these references [45, 46, 47]. The following figure shows a simple circuit to explain the mechanism mentioned above. It must be mentioned that the actual circuit is much more complicated but this figure has been involved for illustration:

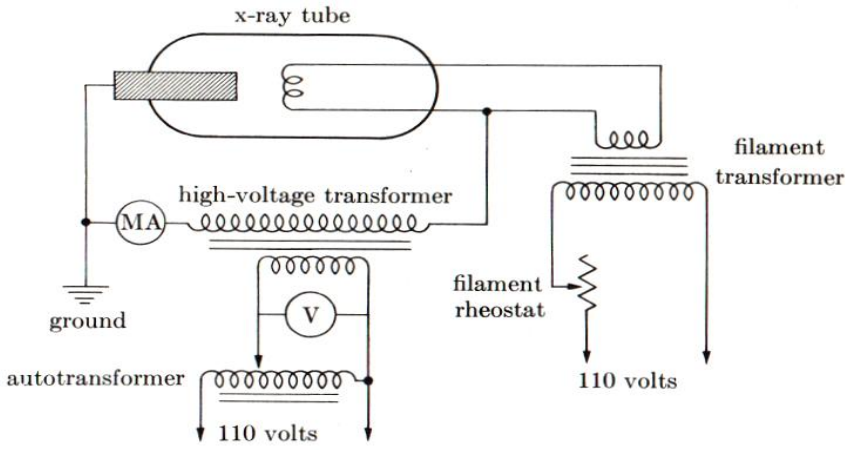

Figure 2-9: Wiring Diagram for the X-ray Tube [45]

In the above figure, the voltage applied to the tube is controlled by the autotransformer which controls the applied voltage to the high voltage transformer. The filament rheostat is controlling the current applied to the filament transformer used to heat up the filament [45].

It was mentioned earlier that, x-rays have been used to study the interior structure of crystalline materials. From this fact, it can be concluded that there is a relationship between the physical properties of x-rays and the geometry of crystals in a material. It is very important to understand the crystals geometry to understand the real

mechanism followed by x-rays. Crystals are built up by periodic repetition of some units, atoms or molecules, which are situated 1 or 2A apart [45]. On the other hand, x-rays are defined as an electromagnetic wave with a wavelength ranging from 0.5 to 2.5A. These two facts can be linked together to introduce a phenomenon called diffraction. It is well known that, diffraction of a wave occurs whenever the wave motion encountered a set of regularly spaced scattering objects. This fact can be true if the wavelength of such wave should be of the same order of magnitude as the repeat distance between the scattering objects [45].

Based on the above approach, by knowing the conditions of the incident wave and diffracted one, the interatomic distance can be studied in a given material. This is the basic of a well known equation called Bragg's Law. This law takes in consideration the fact that, the atoms in any crystals materials are arranged in a specific way to form different planes within the material. The spacing between the planes can be used to identify any given material. The following figure shows the main principle of Bragg's law:

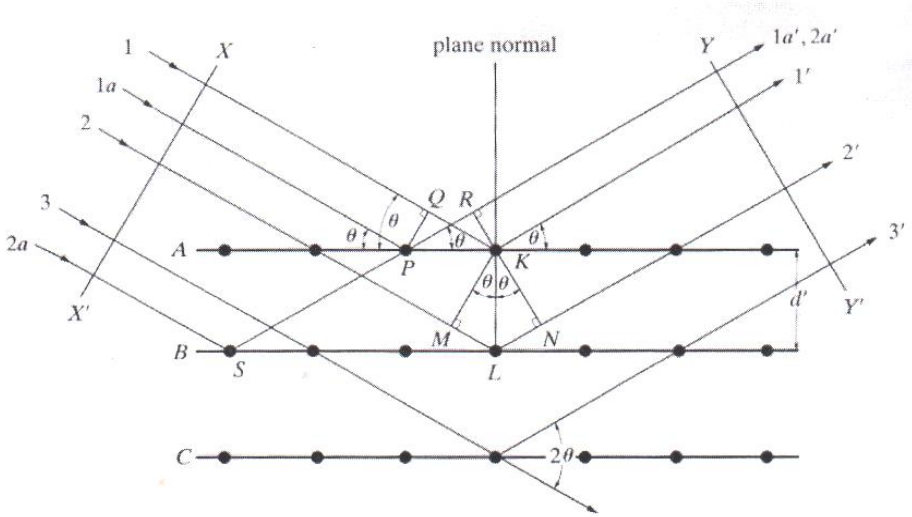

Figure 2-10: Diffraction of X-rays by Atoms [45]

Based on the above diagram, Bragg could mathematically calculate the distance **d** between different planes in a given material. The above diagram showed several parameters that were used in the mathematical derivation that will not be included in

this thesis. The detailed derivation can be found in literature while the final equation that is known as Bragg's law will be shown as it follows:

$$\text{Wavelength of the incident ray} = 2 \times d \times \sin\theta \quad (18)$$

Where, **d** is the spacing between various plans and **θ** is the angle of the incident beam. Experimentally, Bragg's law can be utilized by using x-rays of known wavelength and measuring **θ** to determine the spacing d of various planes in a material. Usually in utilizing the XRD instrument, a spectrum (intensity versus 2θ) with different peaks is generated. A clear peak at a certain angle indicates that a diffraction of x-rays is observed. From the spectrum, the value of **θ** can be recorded and the spacing can then be calculated. Such spectrum can also reveal some other information regarding a given material. In general, XRD spectrum can be useful as it will be illustrated below:

- As it was mentioned earlier, the spacing between various planes can be calculated [45].
- The shape of the peak of the diffracted beam can reveal some important information. For example, the width of the peak (which is measured at intensity equal to half the maximum intensity) increases as the thickness of the crystal decreases. The width of the peak also gives an indication of the imperfection in the arrangement of the crystals. The imperfection can be a result of a broken crystal in the whole structure or the presence of stresses inside the structure leading to disordering generating a broader peak [45].

2.2.3 Scanning Electron Microscope (SEM)

Scanning electron microscope uses a beam of electrons detected at the specimen and it consists of the electron gun, the lenses and the vacuum system. The SEM is mainly used to study the structure of the surface or near surface of a given sample. In general, SEM consists of tungsten as the electron gun generating an electron beam that is usually accelerated to an energy which is usually between 10 to 30 keV. The electron beam is then subjected to the specimen by using condenser lenses and the scattered

electrons are detected by a detector that is counting the number of the electrons received and connected to a television screen showing the required images [48].

If a beam of electrons is subjected to a thick specimen, it will react with the sample and then different radiations will be emitted back from the sample. Such radiations can be secondary electrons, some of the incident electrons are backscattered and x-rays will also be generated. Each radiation will be detected by the detector in the SEM and will be used in a specific purpose. Considering the first two radiations, the numbers of the electrons of the secondary and the backscattered radiations are known as electron coefficients. Such coefficients depend on the nature of the sample studied and therefore they will present the sample itself [48].

Two main types of images can be possibly generated by SEM as it will be shown below:

- Topographic Images: These kinds of images provide information about the morphology of the surface of the sample. The secondary electron coefficient of the beam emitted from the surface of the sample depends on the morphology of the surface. Based on that, the secondary electrons coming out of the surface can be used to generate images studying the surface morphology of a given sample [48-50].
- Compositional images: the nature of the backscattered electron beam depends mainly on the atomic weight of the sample the beam hits. It has been shown in the literature that, the atomic weight (Z) of the compound studied by SEM and the backscattered coefficient (δ) can be related based on the following equation:

$$\delta = -0.254 + 0.016Z - 1.86 \times 10\text{-}4\ Z^2 + 8.3 \times 10\text{-}7\ Z^3 \quad (19)$$

CHAPTER 3

3 EXPERIMENTAL PROCEDURES AND APPARATUS

3.1 Materials and Instruments

This part summarizes all equipment and materials which were utilized in this study. Table 3-1 lists all equipment as shown below:

Table 3-1 Equipment list

No.	Equipment	Manufacturer
1	Plasma Spray System 9MBM	Sulzer Metco
2	Solution Plasma Spray II Delivery System	Inframat Corporation
3	Potentiostat Model 236A	PerkinElmer
4	Potentiostat Model 283	PerkinElmer
5	Salt Spray	Sheen
6	Cold cutting – Secotom 10	Struers
7	Autopolisher – LaboPol – 5	Struers
8	Ultrasonic Cleaner 1510	Bransonic Corporation
9	Scanning Electron Microscopy (SEM), Q400	FEI
10	X-ray diffractometry (XRD)	Pert Pro PaNalytical

The materials components that were utilized in this master thesis study are summarized in the following table:

Table 3-2 Materials list including chemicals and suspensions

No.	Material	Manufacturer
1	Aluminum nitrate nonahydrate $Al(NO_3)_3.9H_2O$	Sigma Aldrich
2	Sodium chloride NaCl	Fisher
3	Allegro/Largo suspension	Struers
4	MD-Dac	Struers
5	DiaPro NapB1	STRUERS
6	Polyurethane sealant (Gloss type)	Sherwin-Williams Diversified
7	EpoFix Resin	Struers
8	EpoFix Hardener	Struers
9	CoCrAlY Powder (Metco 66 FN-S)	Sulzer Metco

The following parts will focus on the methodology of the coating process, testing of the selected samples and characterization step.

The selected substrates in this study were carbon steel with dimension of about 70 X 23 X 3 mm as shown in figure 3-1.

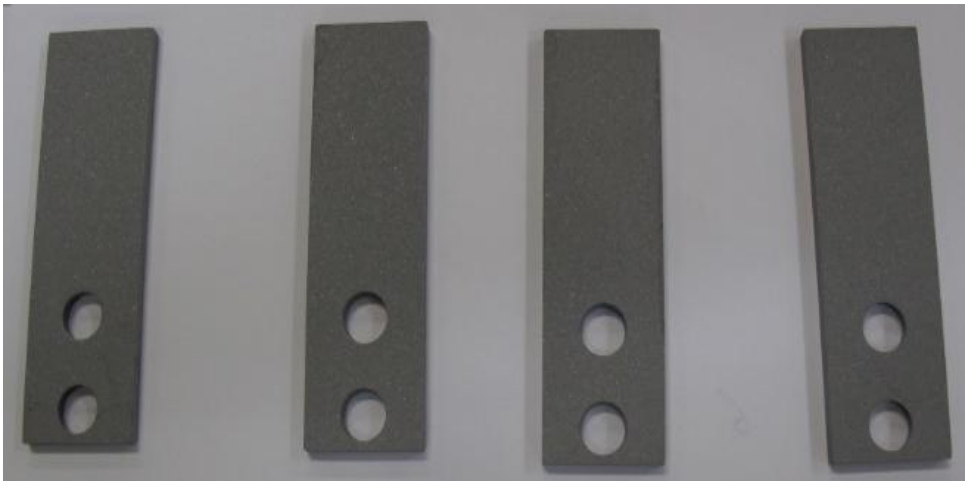

Figure 3-1 Example of some of the used carbon steel substrate

3.2 Samples preparation and Coating deposition

This is the main part of this master thesis study. It consists of three main sections as described below:

- Preparation of aluminum nitrate solution (($Al(NO_3)_3.9H_2O$)
- Surface preparation of carbon steel substrate
- Plasma spray coating deposition by using SPS system

3.2.1 Preparation of aluminum nitrate solution

The first step in this work is to prepare aluminum nitrate solution ($Al(NO_3)_3.9H_2O$ in 3 liters distilled water and mix the solution in a baker for about 30 minutes and at agitation speed of around 300 rpm to ensure full mixing and therefore get homogenous solution. 183 g/L was prepared by mixing 550 g aluminum nitrate in 3 liters of distilled water. In the same way, 283 g/ L was prepared by adding 850 g of aluminum nitrate to 3 liters of distilled water and 375 g/L was prepared by adding 1125 g aluminum nitrate to 3 liters of distilled water. These three different concentrations were already proposed in this master thesis proposal. Therefore, the final concentrations were as follows:

183 g/L

283 g/L and,

375 g/L

After preparing all required solutions, they stored in a very clean plastic bottles to avoid contamination with impurities.

3.2.2 Surface preparation of carbon steel substrate:

After preparing all solutions, the grit blasting steps comes next since it is highly recommended to spray the coating during first 30 minutes after grit blasting step to avoid contamination or oxidation problems. As mentioned in chapter one, the surface preparation is so important in order to get adhered coating on the substrate. The surface of the substrate should be rough enough to create rough areas on the top of the substrate which have the ability to allow the spray coating to mechanically bond with the surface of the substrate. This task was achieved by doing grit blasting on all substrates with using aluminum oxide grit which has 300 micron in size. After that, all substrates were kept in a prepared desiccator under vacuum to prevent oxidation process to take place since oxidation layer might affect the adhesion of the coating and act as barrier between the substrate and coating layer.

After insuring the readiness of the solution and CS substrates, then the coating process can be started.

3.2.3 Plasma spray coating deposition by using SPS system:

prior to start applying the aluminum oxide coating, all main components of plasma spray system (i.e. dust collector, power supply, heat exchanger system, control unit and powder feeder)should be switch on in order to start preheating the substrates and apply thin film of CoCrAly as a bond coat. Table 3-3 summarizes the operating parameters of plasma spray system.

Table 3-3 Plasma spray system operating parameters

Power supply (KW)	Spray distance (mm)	Powder feeding rate (g/min)	Number of preheating passes	Number of spray passes	Rotating table speed (rpm)
37 - 38	102	30	180	180	60

The main purpose of preheating step is to narrow the temperature gap between the substrates and the applied coating to avoid thermal expansion for the coating layer. After finishing the preheat step the system starts to apply thin layer of the bond coat. This bond coat was applied in order to promote surface adhesion and also, to provide layer which has thermal expansion coefficient close to ceramic coating. Thereafter, SPS cylinder feeder should be filled with enough amount of the aluminum nitrate solution. Then the compressed air valve should be open and adjusted at 40 psi to push the liquid through the connected hose and directly injected the solution on the flame of plasma.

Three different flowrates were used in this study at 30 ml/L, 50 ml/L and 70 ml/L. These flowrates was adjusted based on the calibration curve as shown in figure 3-2 below. This curve was developed internally for the purpose of this work in accordance to the manufacturer procedures. The reason of developing this calibration curve is to get accurate readings at 40 psi tank pressure.

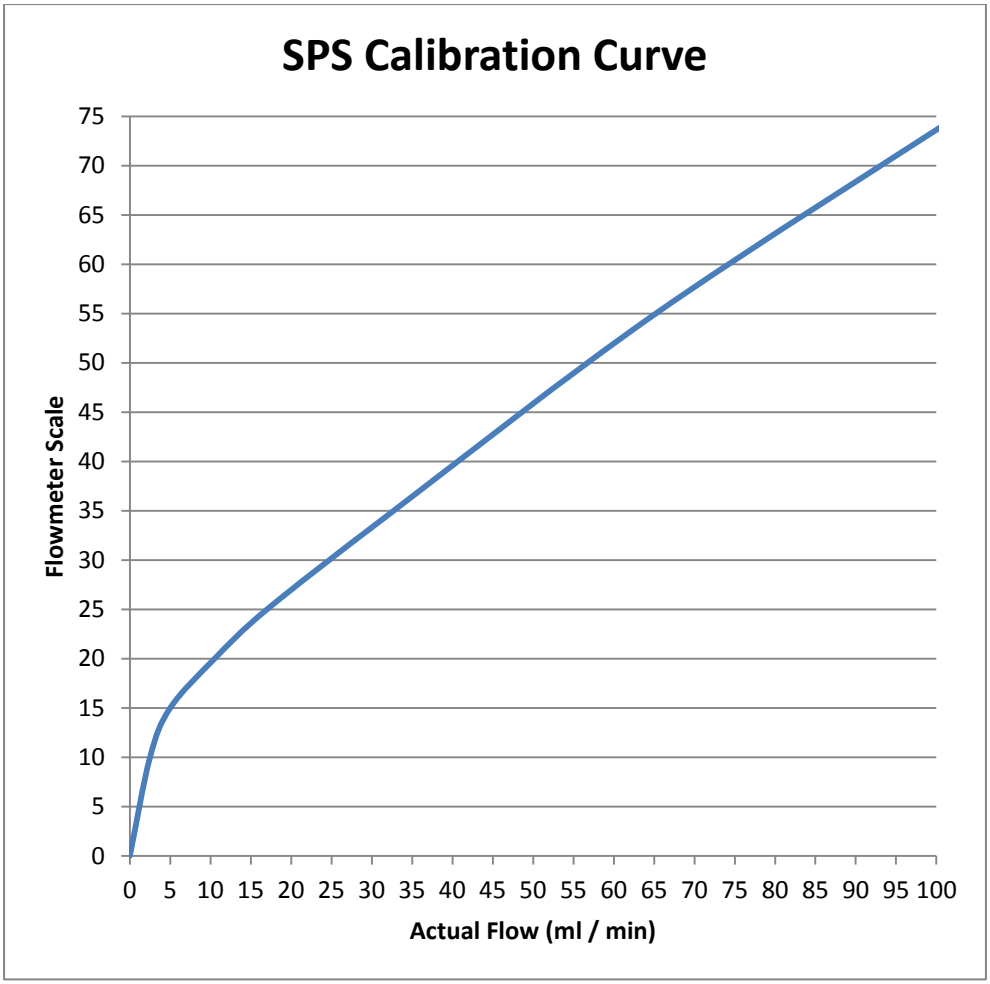

Figure 3-2 SPS Calibration Curve

The solution will definitely, oxidize due to high temperature and converted to ceramic coating with white color. Table 3-4 summarizes the operating parameters for SPS system.

Table 3-4 SPS operating parameters

Power supply (KW)	Spray distance (mm)	Feeding rate (ml/min)	Number of spray passes	Solution concentration (g/L)	Rotating table speed (rpm)
38	50	30, 50 and 70	180	375, 283 and 183	60

The aluminum oxide coating systems parameters and quantity are summarized in table 3-5 below.

Table 3-5 Al_2O_3 coating systems parameters

Concentration (g/L)	183			283			375		
Flowrate (ml/min)	30	50	70	30	50	70	30	50	70
Number of samples	4	4	4	4	4	3	4	4	4

3.3 Methods of evaluation and Characterization

After completing the coating process, only selected samples were tested and characterized. The selected samples have been divided into two groups. The first group was exposed to salt spray environment while the other group were examined as dry films without exposure to salt spray environment. A thin film sealant was proposed to be sprayed on the top of salt spray samples in order to cover the porosity and to be part of the coating system. The sealant material was polyurethane as shown in figure 3-3. Figure 3-3 shows some samples which have a thin layer yellowish color of polyurethane which acts as a sealant. Table 3-6 below summarizes all samples which were exposed to salt spray environment.

Figure 3-3 two carbon steel samples with Al_2O_3 coating and sealant

Table 3-6 Coated samples that were exposed to salt spray environment.

Sample No.	**Concentration (g/L)**	**Flowrate (ml / min)**	**Remarks**
1	375	70	Aluminum oxide coating with sealant
2	375	50	Aluminum oxide coating with sealant
3	375	30	Aluminum oxide coating with sealant
4	283	50	Aluminum oxide coating with sealant
5	283	30	Aluminum oxide coating with sealant
6	183	30	Aluminum oxide coating with sealant
7	No coating	NA	Bare steel with sealant

The salt spray cabinet was operated at 35 ^{o}C and 25 psi operating pressure. The salt content was 3.5 wt% and for reproducibility, two samples from each run were exposed to same condition. AC Impedance test was conducted on each sample before

the exposure to the salt spray environment as dry film and during the exposure in order to measure the pore resistance value for each sample. Figure 3-4 shows the main components of AC Impedance.

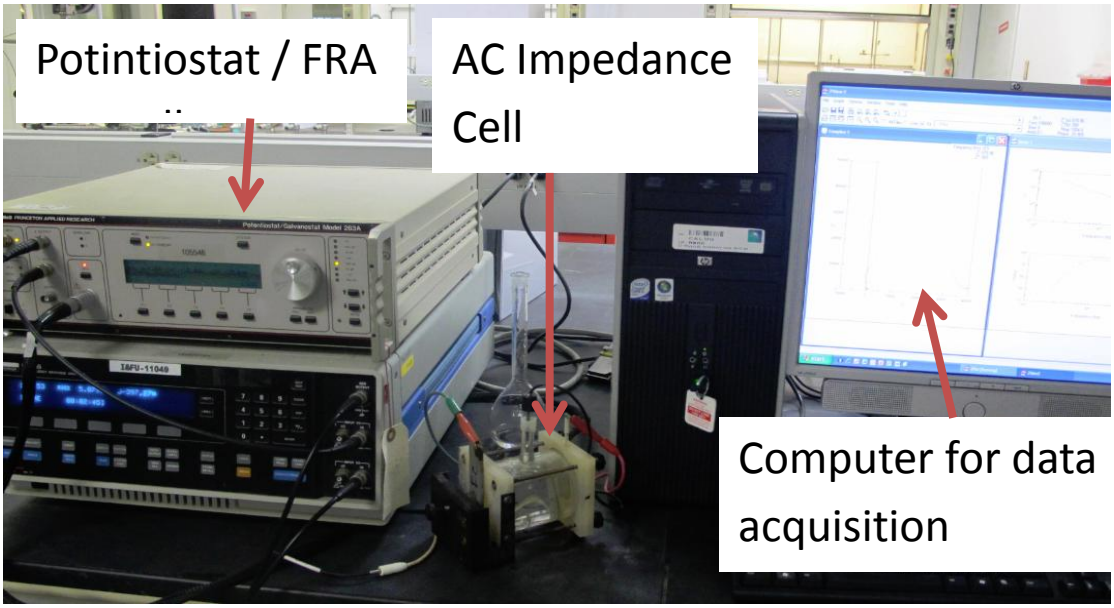

Figure 3-4 Main components of AC Impedance

The main components as shown in the figure 3-4 above are:

1 : AC Impedance cell

2: Potentiostat unit (main controller)

3: Computer for data acquisition

In addition, several samples were metallographically analyzed start with cutting, grinding, polishing and mounted in order to prepare them for SEM and XRD analysis. This part of work was done in accordance to Struers recommended metallography procedures. These procedures were developed by Struers Company especially for thermal spray coating samples.

The selected samples are shown in table 3-7.

Table 3-7 selected samples for SEM and XRD analysis

Sample No.	**Concentration (g/L)**	**Flowrate (ml / min)**	**Remarks**
1	375	70	Aluminum oxide coating
2	375	50	Aluminum oxide coating
3	375	30	Aluminum oxide coating
4	283	30	Aluminum oxide coating
5	183	30	Aluminum oxide coating

CHAPTER 4

4 RESULTS AND DISCUSSION

4.1 Introduction

This chapter will summarize all results obtained in this study. The results includes aluminum oxide coatings at different conditions and also, includes SEM and XRD characterization results which were conducted for selected samples only. In addition, the results will include AC Impedance data with more focus on bode diagram for each set of the experiment. The coated samples consist of nine sets with different parameters in addition to two samples from bare carbon steel. As mentioned earlier in this report, the plasma spray system was utilized to produce the aluminum oxide coating for the purpose of this MSc thesis study and it has the capability to produce four samples at one run and same parameters which is required for reproducibility. All spray processes was operated automatically by using robotic program.

4.2 Visual Inspection

A total of 35 carbon steel samples were coated using aluminum oxide nano-structured coating sprayed by using plasma spray system and solution plasma spray feeder.

The next figures show bare steel samples and the applied aluminum oxide nano-coating on carbon steel samples.

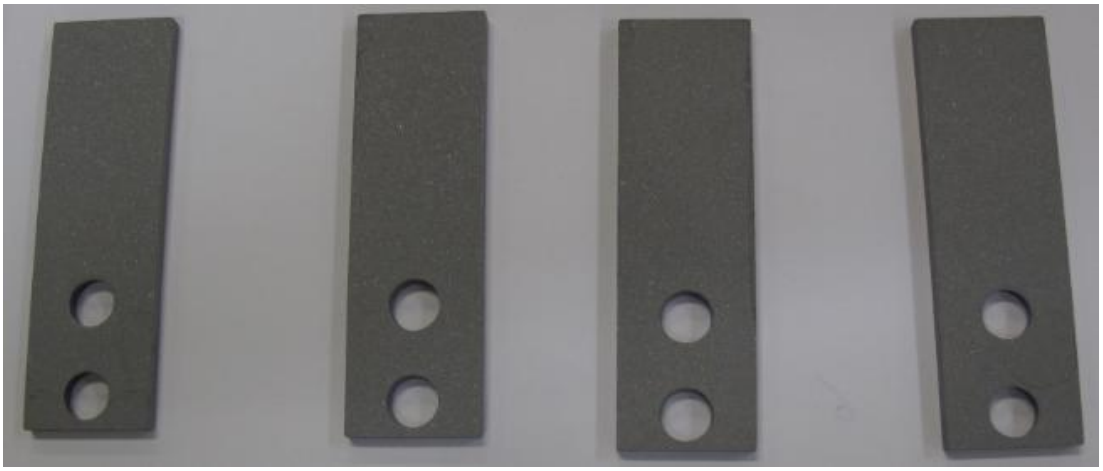

Figure 4-1 Gritblasted carbon steel samples before coating.

The above samples were gritblasted to provide rough surface which is required prior to apply the required coating. This task is necessary in order to promote the adhesion of the coating.

However, some samples show good coating in terms of adhesion and bonding while the aluminum oxide coating layer delaminated from other coated samples. The figure below show the coated samples at different conditions.

- At flowrate of 70 ml/min and 375 g/L concentration (set 1):

Figure 4-2 Set 1 with Aluminum oxide coating

The figure above shows photo of samples 3 and 4 which are identical and represents the whole samples in the same run. It shows white color with uniform aluminum oxide coating layer. However, it has been observed that this coating at above parameters did not show good adhesion as we noticed later after producing the coating. The coating delaminated from some substrate in same run due to high flowrate and perhaps the fluctuating in the flowrate quantity during the spray process.

- At 50 ml/min and 375 g/L (set 2)

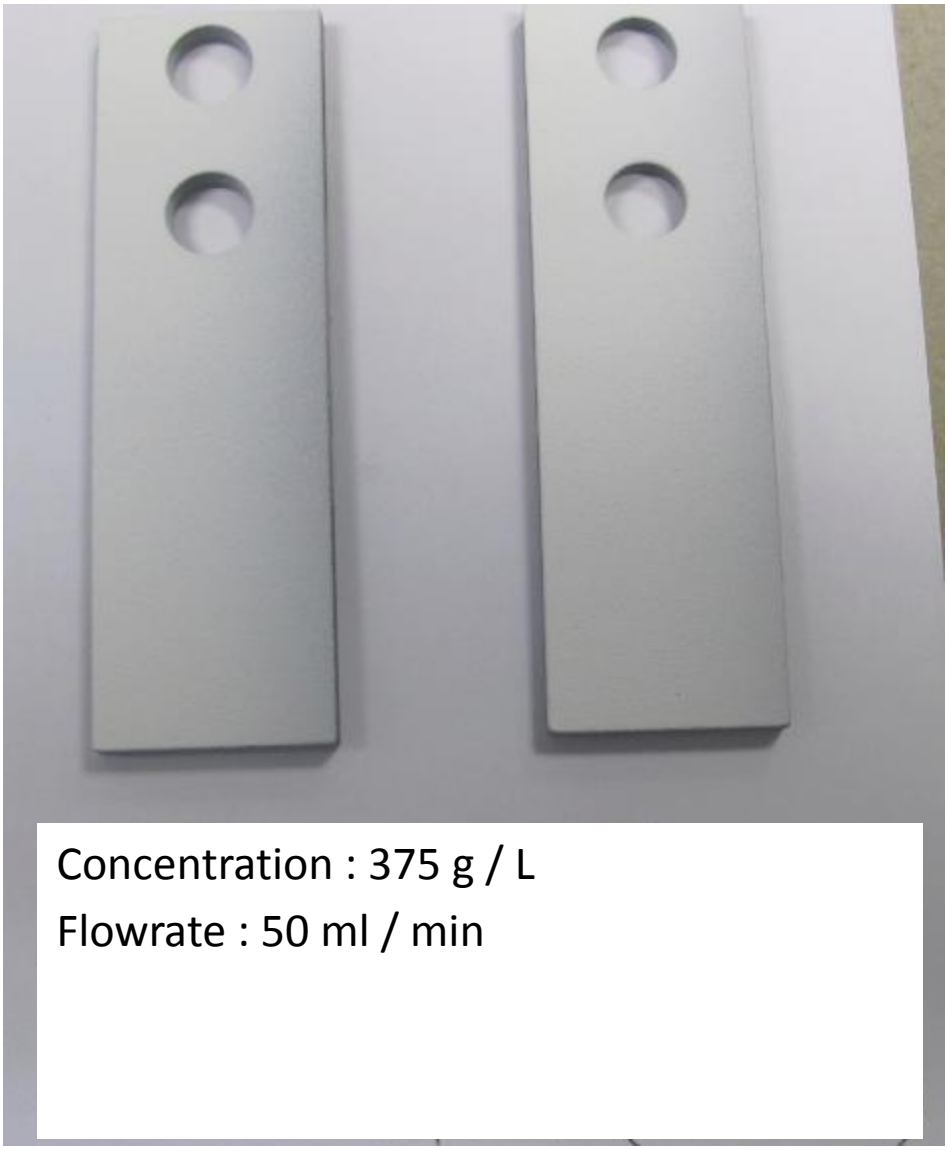

Figure 4-3 Set 2 with Aluminum oxide coating

The figure above shows the aluminum oxide coating sprayed at the above parameters. This photo was taken for samples 7 and 8 for the same run and therefore, they represent the whole samples in the same run. However, this coating system shows good adhesion comparing to set 1 system.

- At 30 ml/min and 375 g/L (set 3)

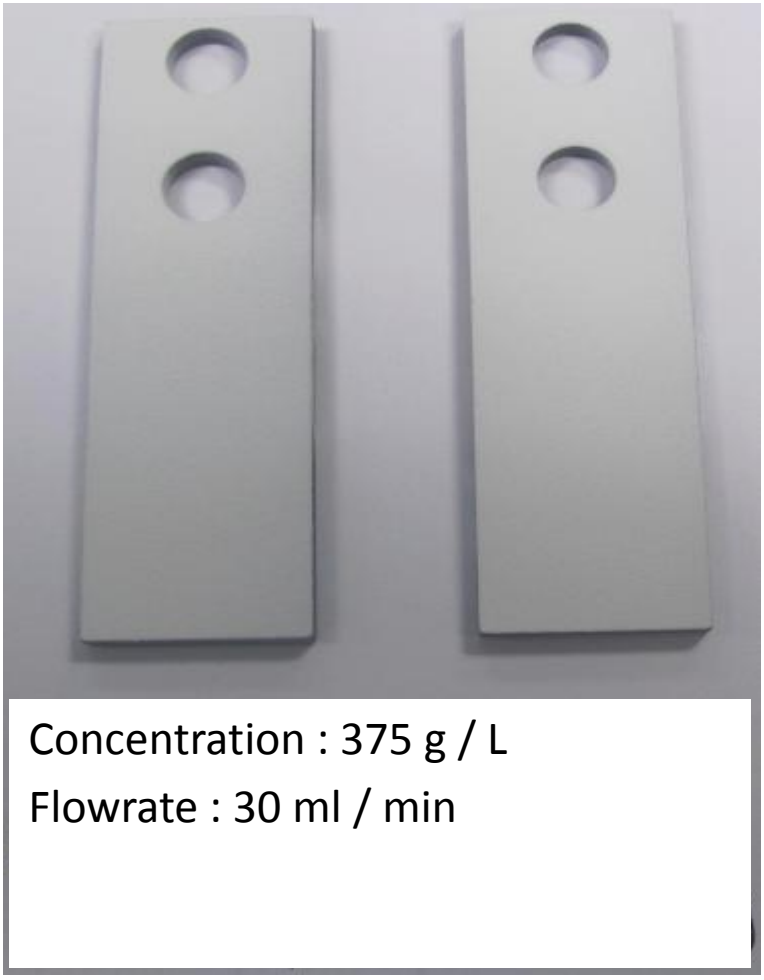

Figure 4-4 Set 3 with Aluminum oxide coating

The figure above shows the aluminum oxide coating sprayed at the above parameters. This photo was taken for samples 10 and 12 for the same run and therefore, they represent the whole samples in the same run. However, this coating system shows better adhesion than set 1 system.

- At 70 ml/min and 283 g/L (set 4)

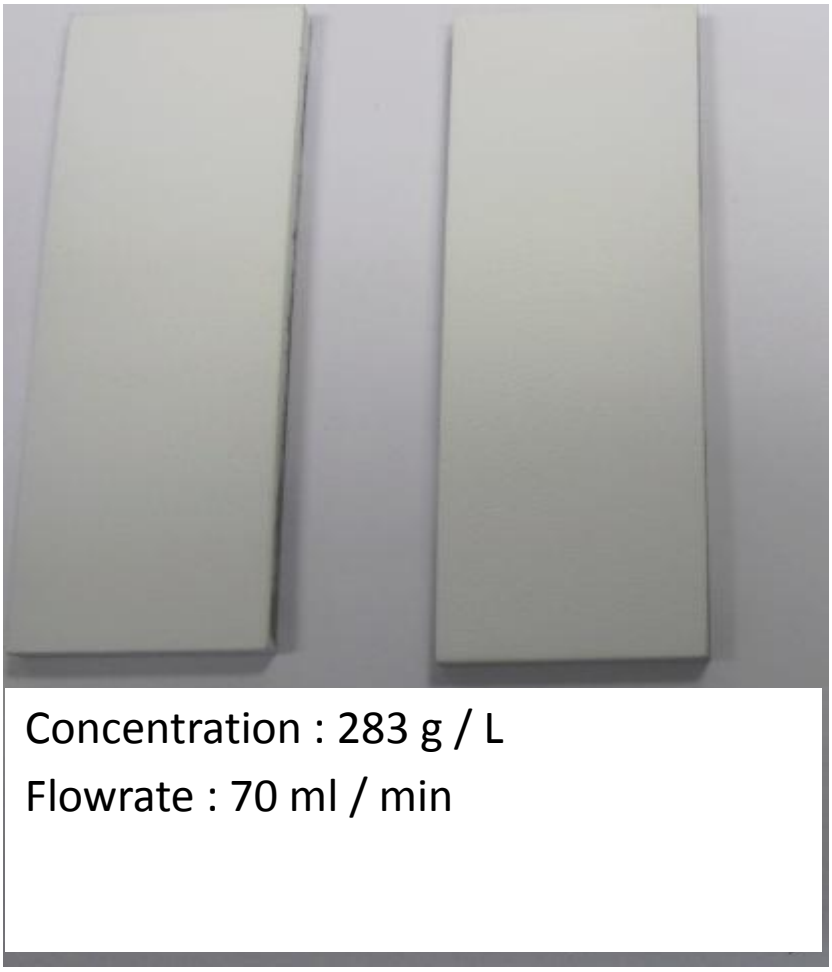

Figure 4-5 Set 4 with Aluminum oxide coating

The above aluminum oxide coating system at 70 ml/min flowrate and 283 g/L concentration (850 g/3L) did not show a good adhesion behavior since the whole coating delaminated after a while as illustrated in the following figure:

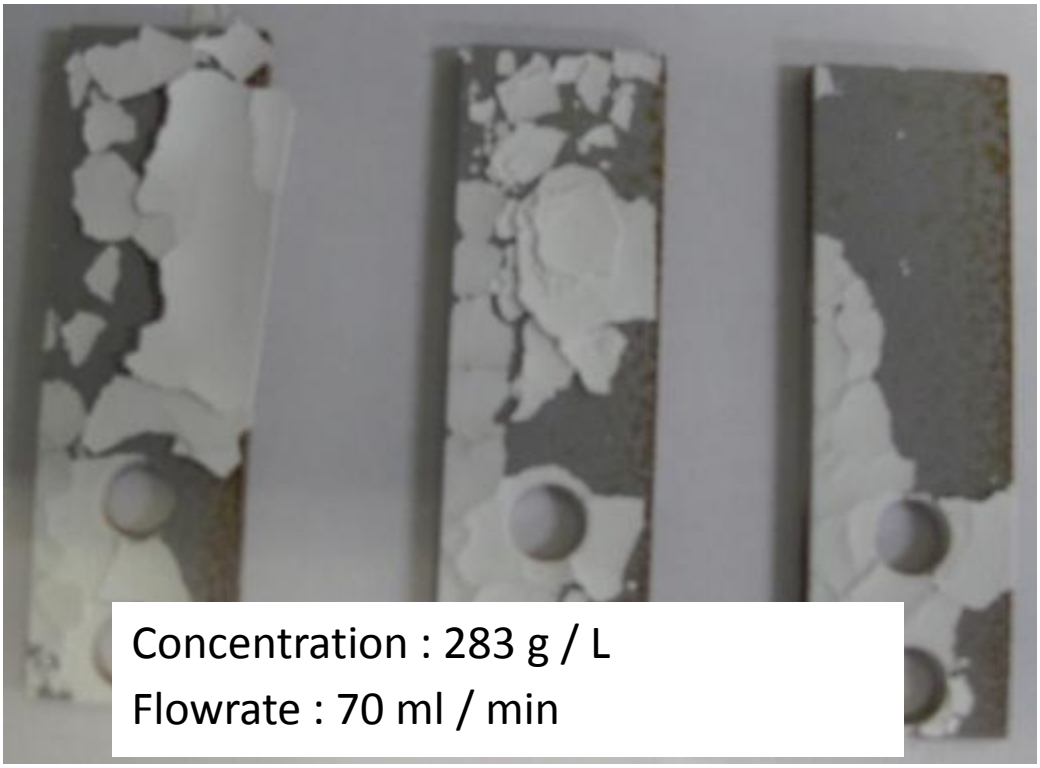

Figure 4-6 Set 4 after aluminum oxide coating delamination

This test was repeated two times at same parameters but it gives same results. Therefore, coating spray at 70 ml/min flowrate and 283 g/L concentration is not recommended since it shows bad adhesion and the corrosion products starts to accumulate on the surface of the target substrate which is an indication that this coating system at the parameters mentioned above is not a protective coating against corrosion.

- At 50 ml/min and 283 g/L (set 5)

Figure 4-7 Set 5 after coating process

This coating process was repeated two times but it gave same performance. The coating started to delaminate just after coating process when it became cold. This can contribute to the thermal expansion of the aluminum oxide coating and due to higher flowrate with less concentration. Also, flowrate fluctuating during the spray process can be considered as a reason of this delamination since the rapid increase in the solution flowrate during the process will definitely introduce more cold liquid into spray stream. Therefore, a rapid decrease in the temperature is expected when this cold amount of solution hit the surface of the sample. Therefore, after

keep spraying more hot solution on the surface of the sample will create temperature difference and as a result, the adhesion of the coating will be affected. This process will push the coating layer to delaminate from the surface and then corrosion process will start as seen in sample 18. These two samples in the above figure represent the whole samples in the same run. Therefore, this coating system cannot be considered as protective coating against corrosion.

- At 30 ml/min and 283 g/L (set 6)

  The figure below shows representative samples which was coated by aluminum oxide.

Figure 4-8 Set 6 after coating process

The above coating samples show good adhesion comparing to the previous sets. It was uniform and well adhered to the substrate.

- At 70 ml/min and 183 g/L (set 7)

  This coating system was delaminated immediately after the spray process as shown in the figure below.

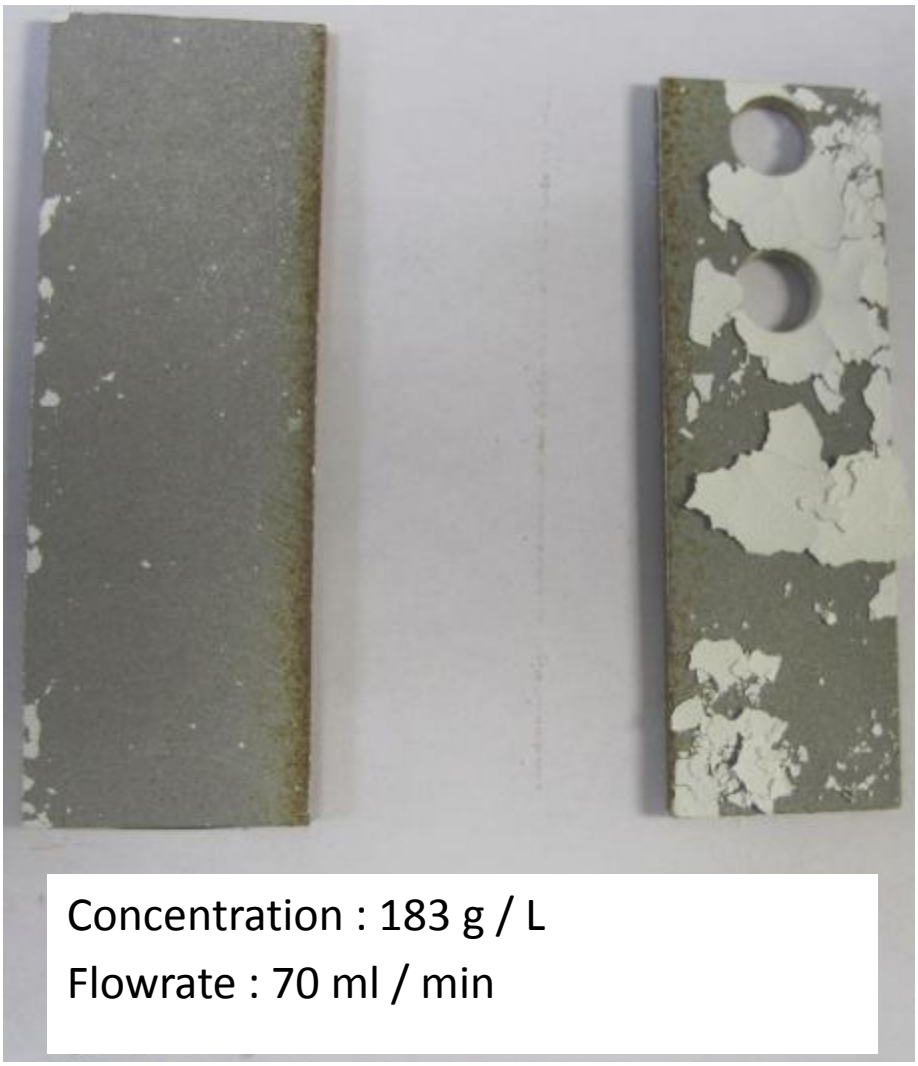

Figure 4-9 Set 7 after coating process

These two samples represent set 7. In this coating system, the concentration of the solution was decreased by 35%. Therefore, more amount of water just hit the surface

of the substrate and lower the temperature of the surface. Hence, when the converted aluminum oxide coating touches the surface of the substrate and due to big temperature gap between the substrate and the upcoming solution, the coating was delaminated because of thermal expansion.

- At 50 ml/min and 183 g/L (set 8)

This coating system was delaminated from the substrate as shown in the figure below:

Figure 4-10 Set 8 coating system

The coating layer was delaminated right after the coating process and the corrosion process started from the edge of the samples. Therefore, this coating system at same

parameters (50 ml/min flowrate and 183 g/L concentration of aluminum nitrate solution) cannot be considered as protective coating against corrosion.

- At 30 ml/min and 183 g/L (set 9)

This coating system was the last set and it shows good adhesion with no indication of delamination even after two months from spray process as shown in the figure below:

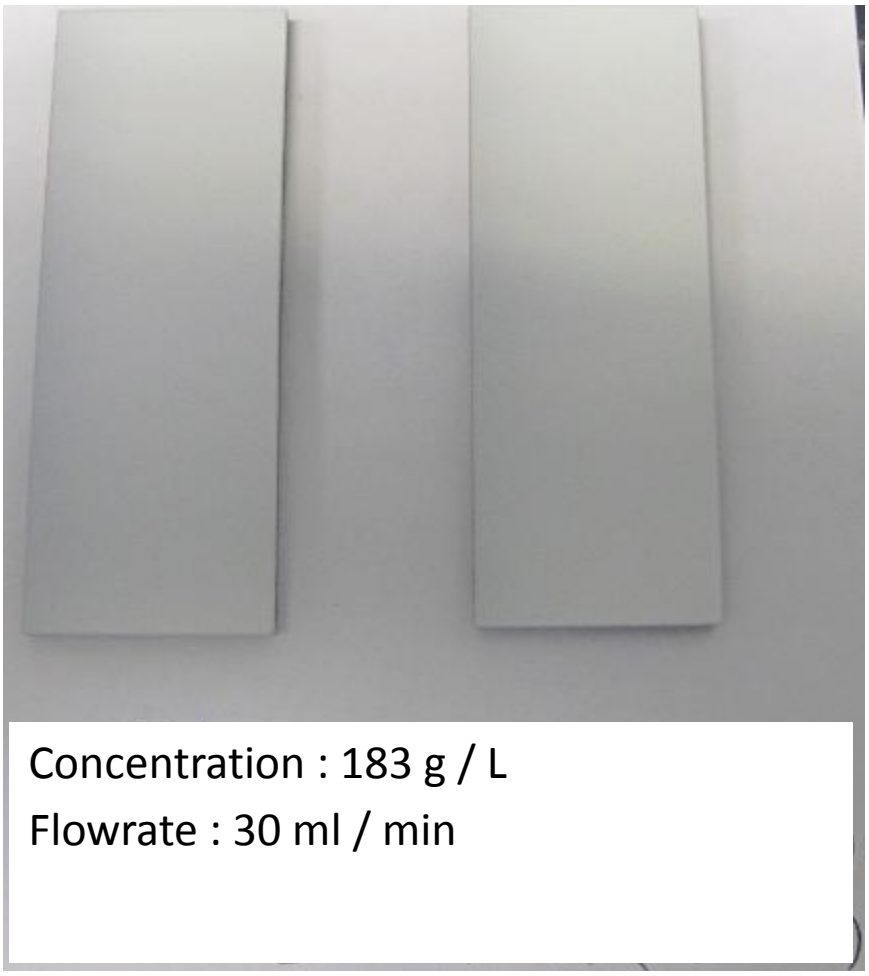

Figure 4-11 Set 9 Aluminum oxide coating

4.3 Salt Spray and AC Impedance

After producing all coating systems, only selected samples were considered in the salt spray test including set 1, 2, 3, 5, 6 and 9 as shown in table 3-6 in chapter 3. The following figures show a comparison of each sample before and after salt spray environment exposure for about 6 weeks.

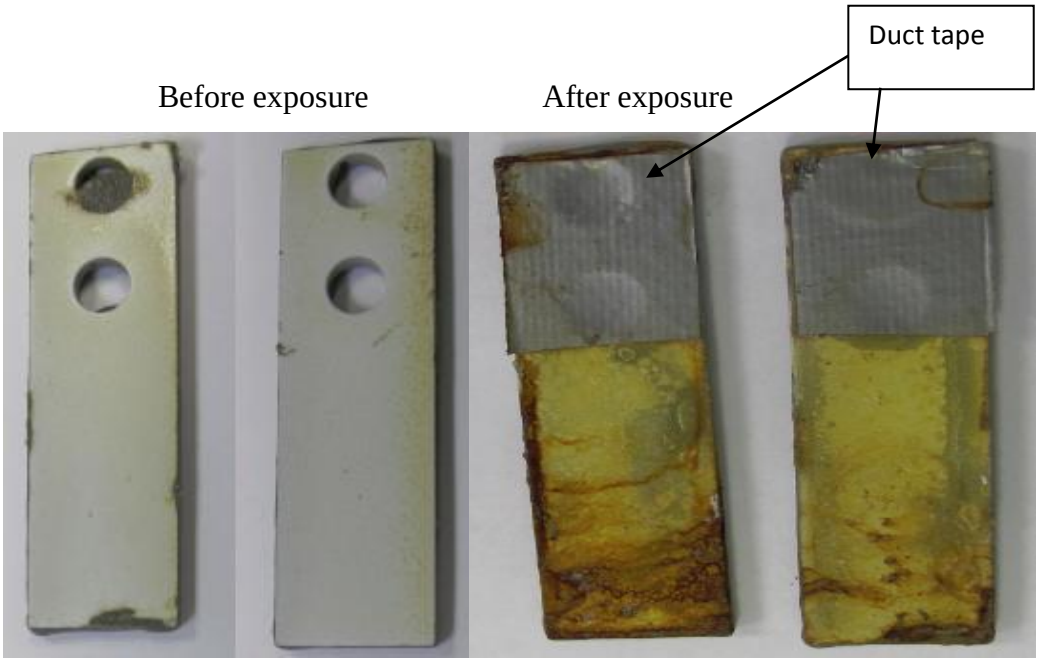

Figure 4-12 Set 1 samples before and after salt spray exposure

It has been clearly noticed that a corrosion process started in the edge of the samples and build up a corrosion layer on the surface of the samples. This corrosion process can contribute to the bad epoxy coverage where belzona epoxy was utilized in all samples just to cover uncoated faces and prevent water from reaching the surface of the substrates. this epoxy was applied on the uncoated faces to make sure no corrosion process can start in the uncoated faces therefore, coated face can be easily inspected if the corrosion process start or not. It appears from the figure above that some corrosion process started at middle and bottom side of the

two samples above and this can reveal that water had reached the surface due to porosity and then allow corrosion process to start. The duct tape shown in the figure above was used just to cover the two holes at top of each sample and prevent water from reaching the surface of each sample.

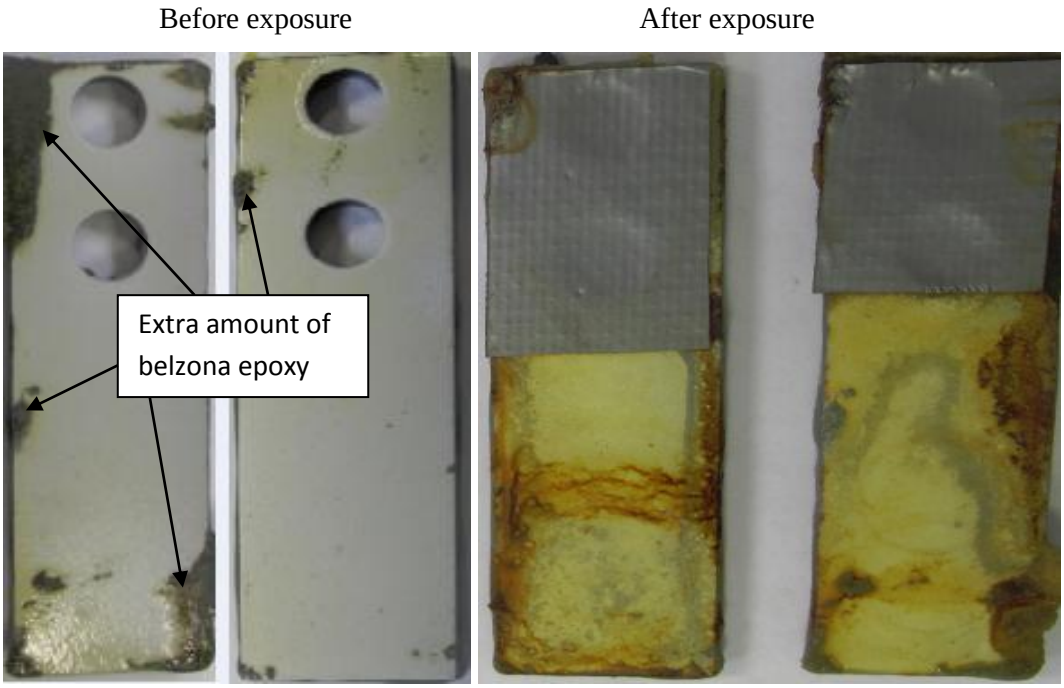

Figure 4-13 Set 2 before and after salt spray exposure

In this coating system, it has observed that this system showed better protection performance against corrosion than set 1. Extra amount of belzona coating reached the coating side however; this amount of belzona epoxy did not damage the coating. The figure below shows that corrosion products appear mainly at the edge of each sample which mean that belzona epoxy was not fully covered for uncoated faces.

Before exposure After exposure

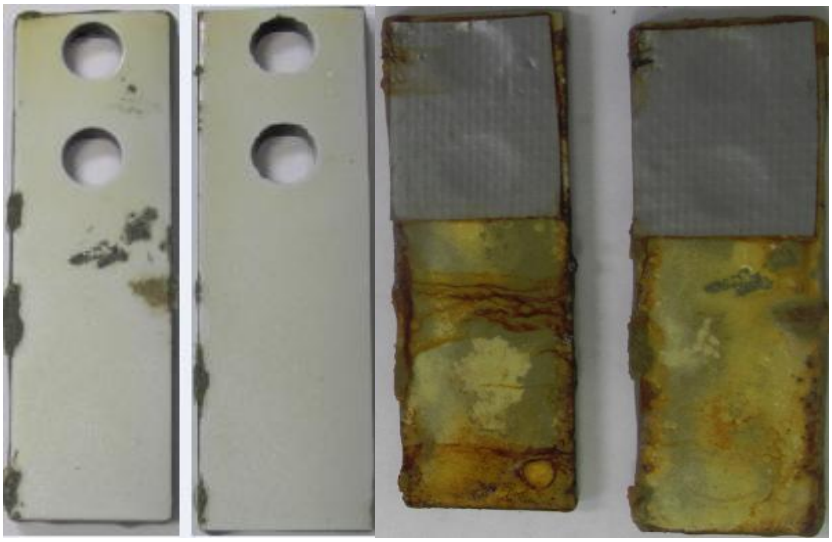

Figure 4-14 set 3 before and after salt spray exposure

This coating system did not show better corrosion performance against corrosion in the aqueous environment than previous 2 sets and corrosion can be noticed at the edge of both samples in the figure above and also, in some spots at the middle of both samples. This corrosion layer appear on the samples due to porosity in the aluminum oxide coating which allow water to reach the surface of the carbon steel substrate.

Set 4 was removed from salt spray test since there was no coating layer on the carbon steel samples. The parameters of set 4 were 70 ml/min flowrate and 283g /L concentration of aluminum nitrate.

The figure below shows carbon steel coated samples before and after salt spray test.

Before exposure After exposure

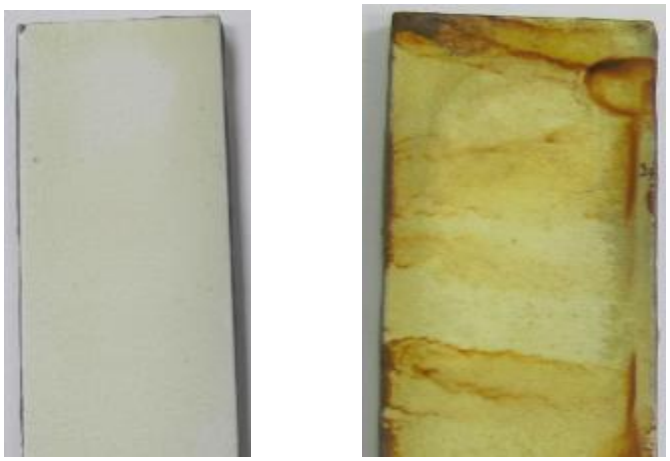

Figure 4-15 set 5 before and after salt spray exposure

Also, this coating system has corrosion products initiated at the edge of the sample between the belzona epoxy and the surface of the substrate. This corrosion products initiation can be contributed to poor coverage by belzona epoxy. Two samples were selected in this set for salt sprat test but one sample was excluded from the test since the coating was removed during removal of duct tape to conduct AC Impedance test. Therefore, only one sample is shown in the figure above.

The next figure below shows some samples in set 6 after and before exposure to salt spray environment

Before exposure After exposure

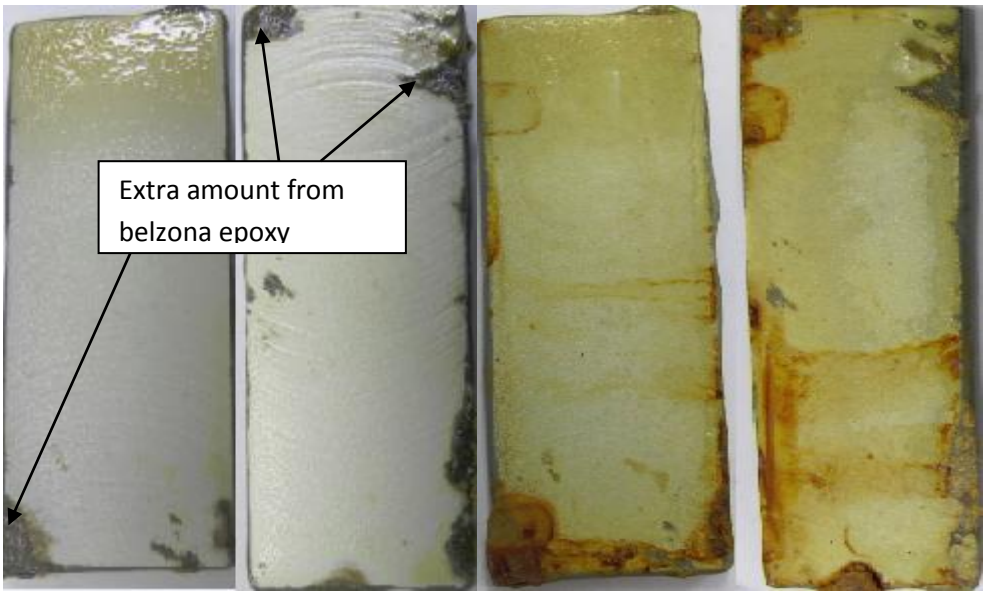

Figure 4-16 Set 6 before and after salt spray exposure

This shows similar performance to the previous set such as set 3. The corrosion products can be observed on the edge of both samples.

Sets number 7 and 8 were not included in the salt spray test since the aluminum oxide coating delaminated and hence there was no coating to inspect or test.

The following figure shows samples from set 9 which is the last set in this study.

Before exposure After exposure

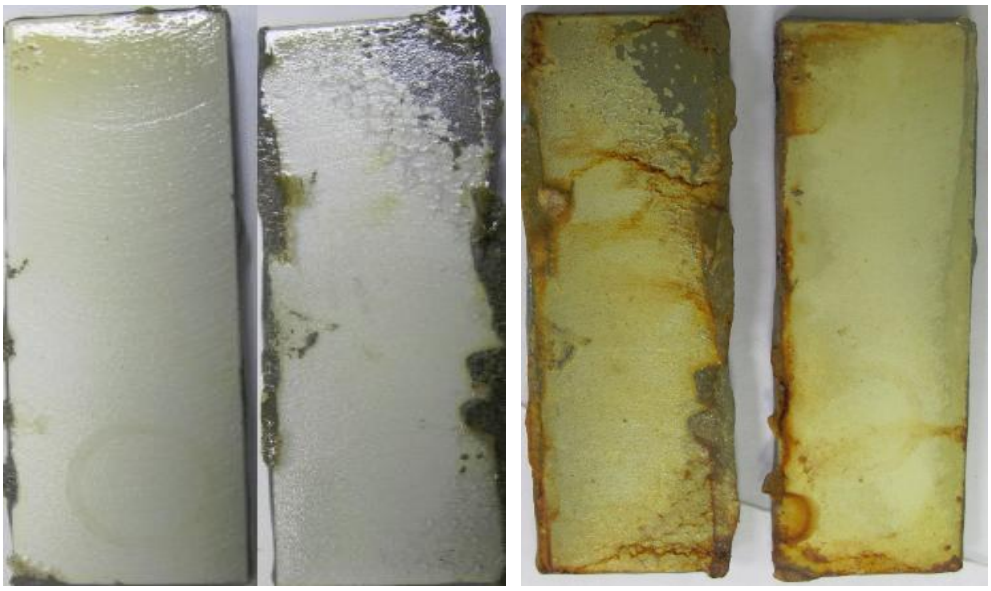

Figure 4-17 Set 9 before and after exposure to salt spray environment

As shown in the figure above, corrosion process initiated at the edge of each samples however, the second sample at the right show better performance than the one in the middle of the figure. This better performance can contribute to the good adhesion in the coating system and excellent coverage for the belzona epoxy which was used to cover uncoated faces.

On the other hand, the bare steel samples without coating but with sealant only, have suffered a severe corrosion on all faces as shown in the figure below.

Before exposure After exposure

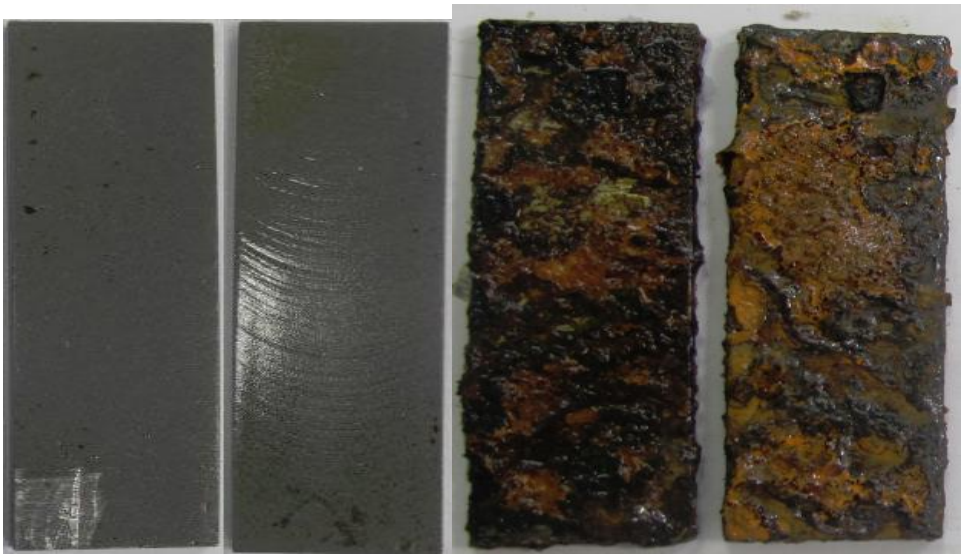

Figure 4-18 Bare carbon steel without coating

As shown in the right hand figure, the corrosion products cover all two samples even in presence of the sealant layer. They have been exposed to same salt spray environment. This is an indication that allows us to conclude that sealant alone with no aluminum oxide coating layer cannot provide a protective layer against corrosion but the previous samples with aluminum oxide coating show better performance against corrosion.

The following part will focus on the AC Impedance test. AC Impedance test was conducted on each sample every day during the first week of the salt spray exposure. The obtained data from AC Impedance can be summarized for each set of samples in the table 4-1 below and the data obtained showed the pore resistance for the coating. The readings in the table represent average of the final readings for five spots in each AC impedance test for each set of sample. All selected sets with their conditions are summarized as follows:

Set 1 (70 ml/min flowrate and 375 g/L concentration)

Set 2 (50 ml/min flowrate and 375 g/L concentration)

Set 3 (30 ml/min flowrate and 375 g/L concentration)

Set 4 (50 ml/min flowrate and 283 g/L concentration)

Set 5 (30 ml/min flowrate and 283 g/L concentration)

Set 6 (30 ml/min flowrate and 183 g/L concentration)

Set 7 (70 ml/min flowrate and 375 g/L concentration with no sealant)

Table 4-1 AC Impedance Data

Day	Set 1	Set 2	Set 3	Set 4	Set 5	Set 6	Set 7	Bare steel
1	9.07E+07	2.41E+07	1.13E+08	4.64E+07	8.06E+07	9.87E+07	5.19E+02	4.98E+07
2	1.77E+05	2.42E+05	2.23E+05	5.57E+05	2.96E+05	1.65E+05	1.47E+02	1.36E+05
4	5.81E+04	2.72E+04	2.01E+04	2.83E+03	7.98E+03	5.50E+03	1.43E+02	2.60E+02
5	4.50E+04	5.18E+04	6.10E+04	4.77E+04	5.67E+04	5.65E+04	8.55E+02	1.58E+02
9	3.37E+04	5.23E+04	6.03E+04	2.20E+04	6.33E+04	4.58E+04	1.50E+02	1.20E+02
10	2.04E+04	5.08E+04	5.18E+04	1.33E+04	5.98E+04	2.95E+04	1.45E+02	9.93E+01
11	1.86E+04	3.05E+04	3.23E+04	3.03E+04	4.03E+04	2.05E+04	1.80E+02	3.72E+02
12	8.69E+03	1.95E+04	1.65E+04	2.14E+04	4.06E+04	2.70E+04	1.47E+02	1.31E+04
16	1.77E+04	2.34E+04	2.60E+04	1.19E+04	3.62E+04	2.58E+04	1.76E+02	9.61E+02
37	2.77E+03	9.43E+03	2.60E+03	6.80E+03	4.14E+04	2.52E+04	3.25E+03	4.05E+01

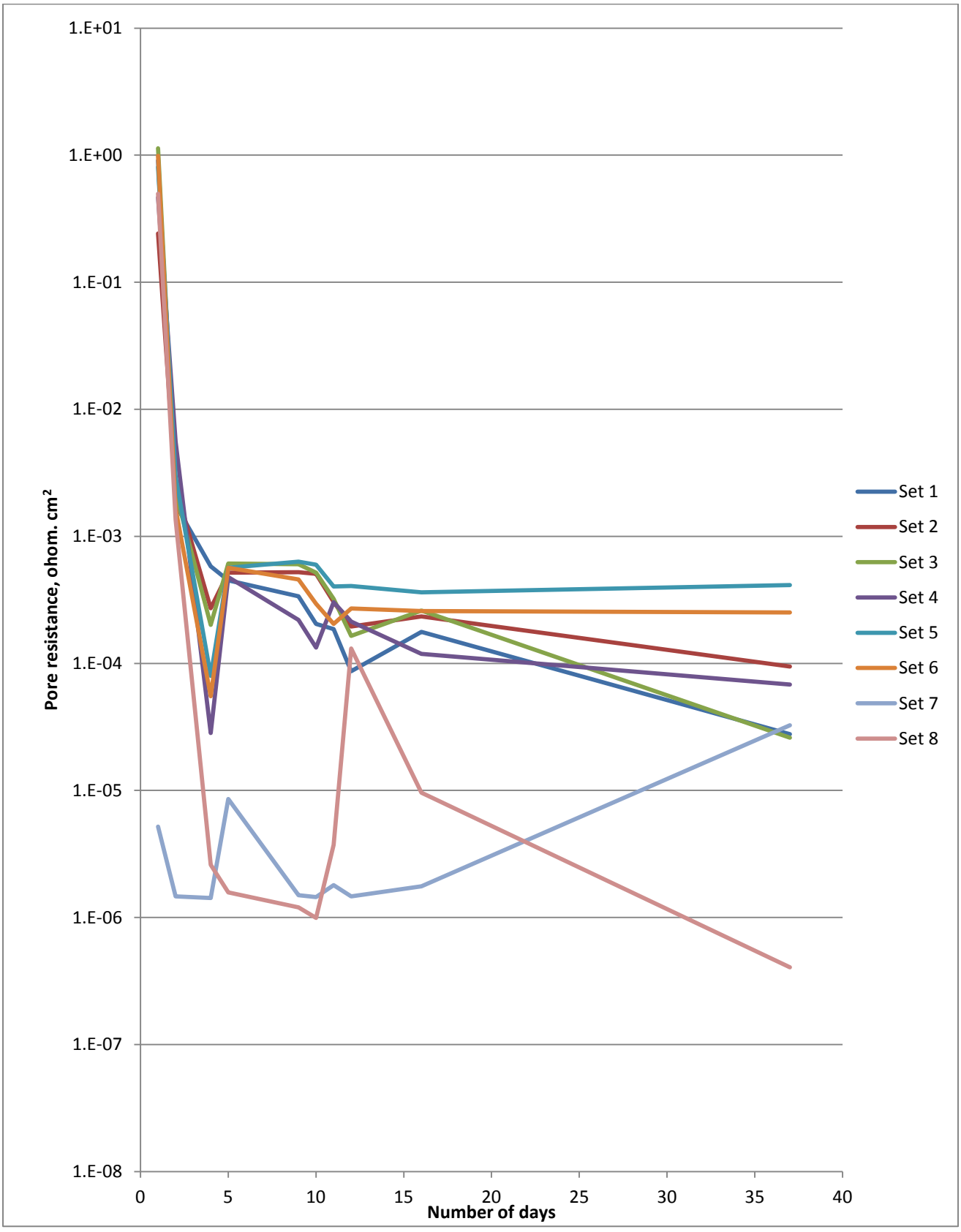

Figure 4-19 AC Impedance Data

The figure above (4-19) shows all data obtained by AC Impedance technique for each set of samples.it shows significant drop in pore resistance reading in the first day. Generally, the main objective of having a coating system on a substrate is to create a very low capacitance with high value of ionic resistance. Accordingly, such coating system will play a major role in hindering the movement of charge leading to low corrosion rate.

The coating capacitance and resistance are highly affected by the present of water in the coating. It is believed that the water will support reducing the ionic resistance of the coating and consequently reducing the efficiency of the coating. Based on that, in evaluating any coating system, the coating capacitance and resistance must be studied. One of the best techniques to measure these two parameters is AC Impedance which was used heavily in this project. Considering the data generated for each coating, it is very obvious that the coating resistances for all coatings were decreasing after 24 hours of exposure. Such sudden drop is a clear indication of a breakdown in the coating. It is well documented in the literature that, the water diffusion inside a coating is usually following three main stages, fast diffusion, saturation and a breakdown in the coating. The first stage takes place during very short period of time followed by the saturation stage where the coating is saturated with water. Such saturation usually does not exceed 2-5 % water in the coating. During these two stages, the coating can still be considered as a good system. The third stage is considered when the water content reaches high level and breakdown in the coating system. At this stage the coating is usually experiencing loss of adhesion, delamination and micro-cracks. This stage is usually spotted out by a sudden drop in

the coating resistance measured by the Impedance which was observed during studying the prepared coatings.

The following figures below show graphs generated by AC impedance technique for each set of samples and also, the comparisons between the bare steel samples and other samples at different flowrates as follows:

- Set 1 at 70 ml/min flowrate and 375 g/L concentration:

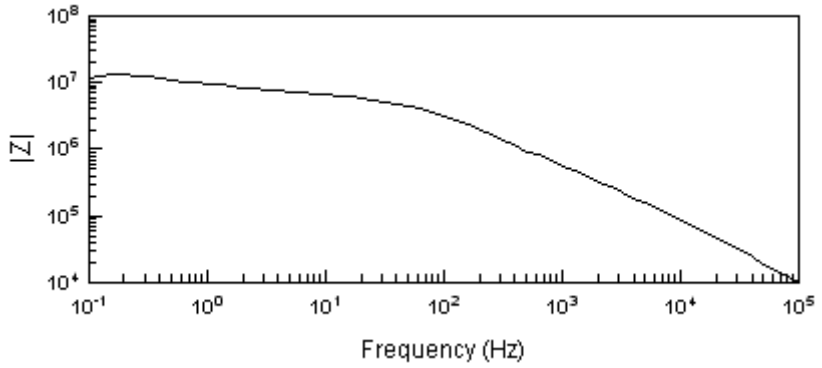

Figure 4-20A Bode diagram for set 1at day 1

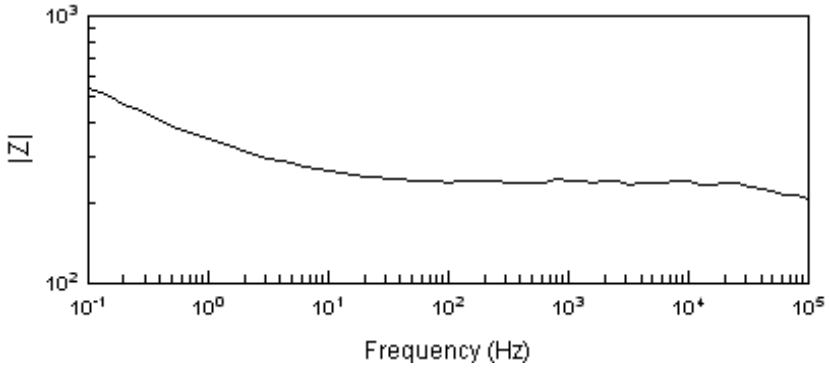

Figure 4-20B Bode diagram for set 1at day 37

The two AC Impedance figures above show the significant drops in the pore resistance reading during period of exposure.

- Set 2 at 50 ml/min flowrate and 375 g/L concentration

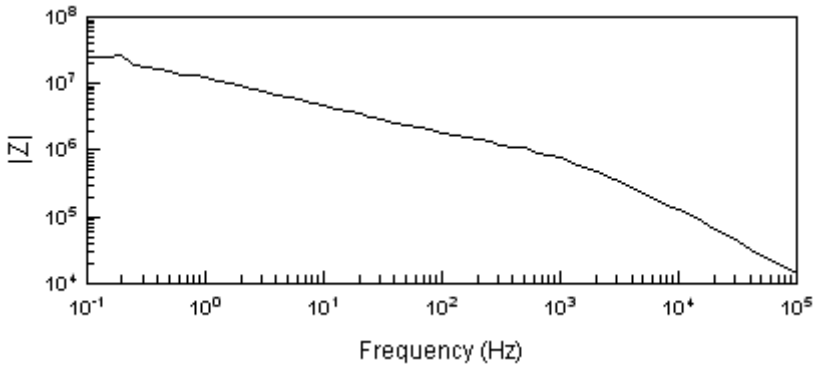

Figure 4-21A Bode diagram for set 2 at day 1

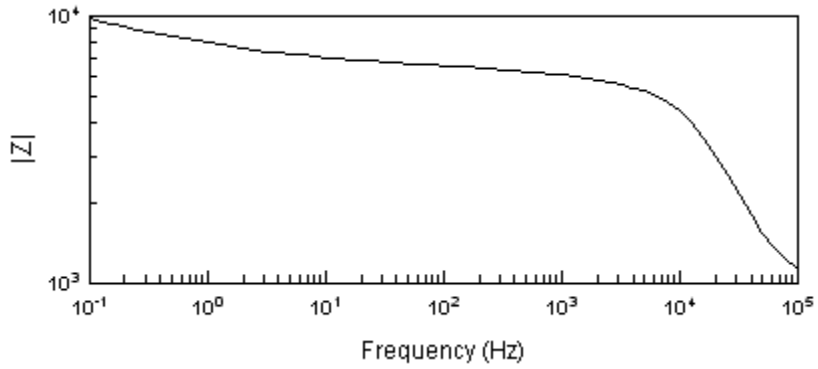

Figure 4-21B Bode diagram for set 2 after 37 days

- Set 3 at 30 ml/min flowrate and 375 g/L concentration

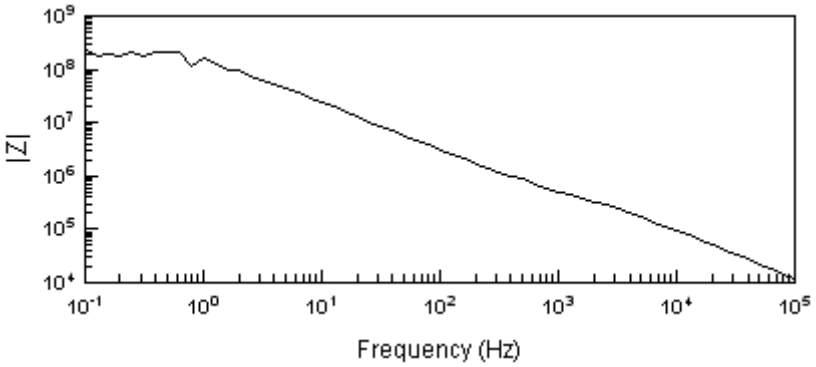

Figure 4-22A Bode diagram for set 3 at day 1

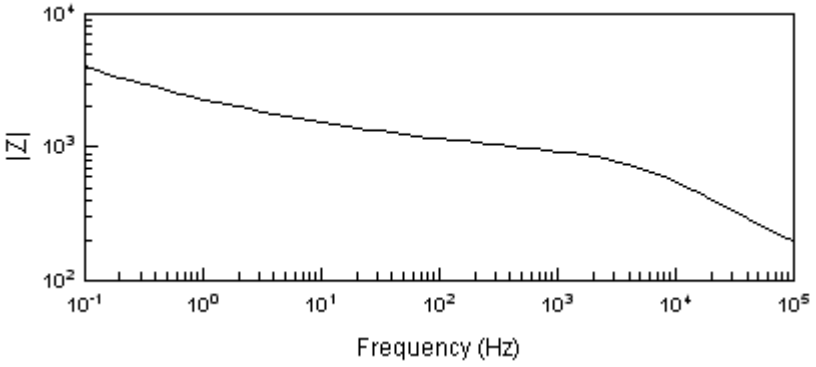

Figure 4-22B Bode diagram for set 3 at day 37

- Set 4 at 50 ml/min flowrate and 283 g/L concentration

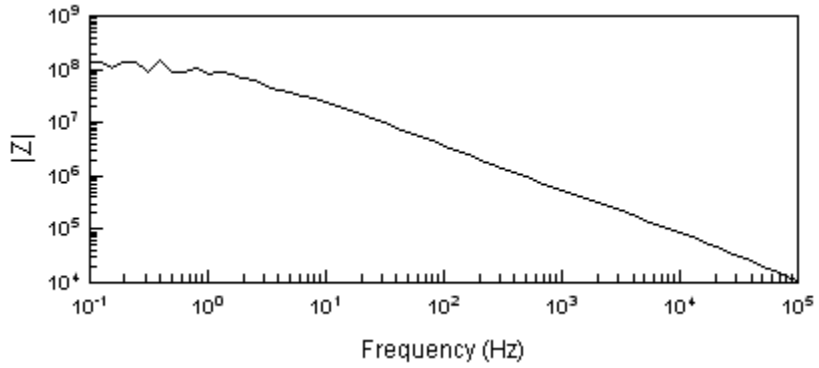

Figure 4-23A Bode diagram for set 4 at day 1

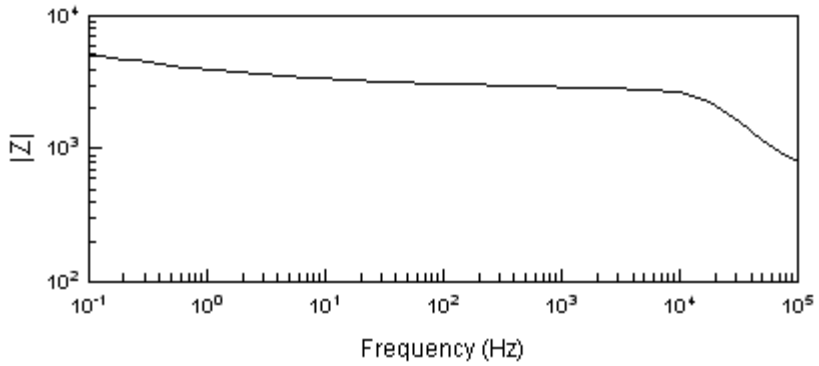

Figure 4-23B Bode diagram for set 4 at day 37

- Set 5 at 30 ml/min flowrate and 283 g/L concentration

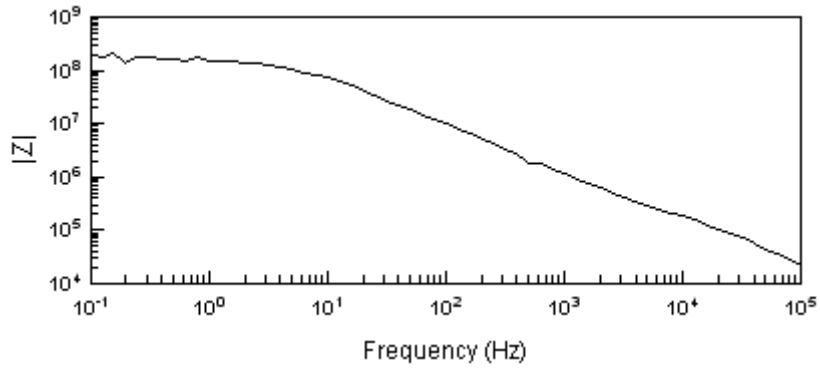

Figure 4-24A Bode diagram for set 5 at day 1

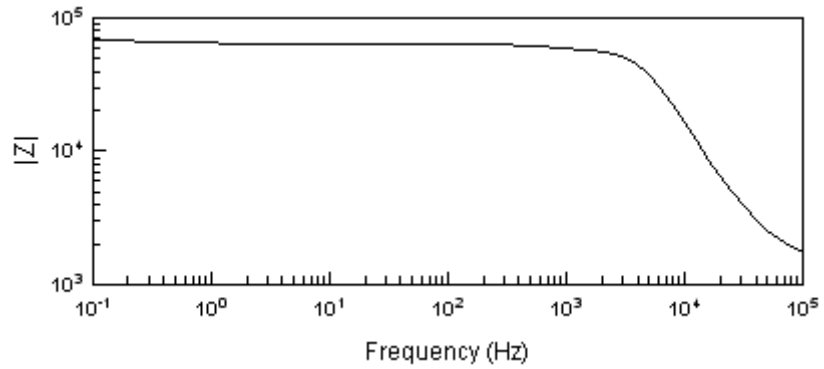

Figure 4-24B Bode diagram for set 5 at day 37

- Set 6 at 30 ml/min flowrate and 183 g/L concentration

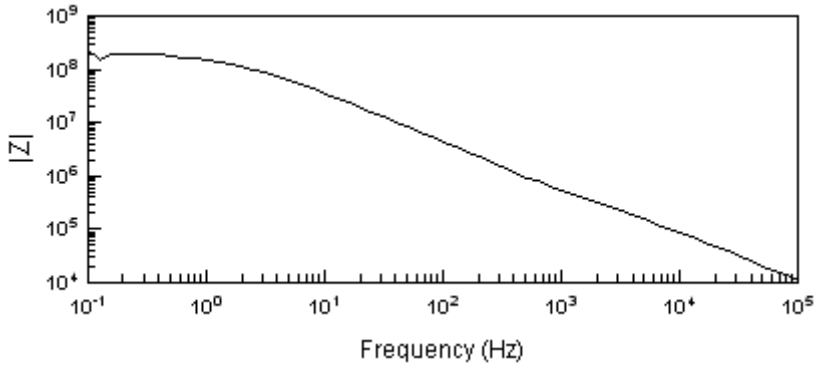

Figure 4-25A Bode diagram for set 6 at day 1

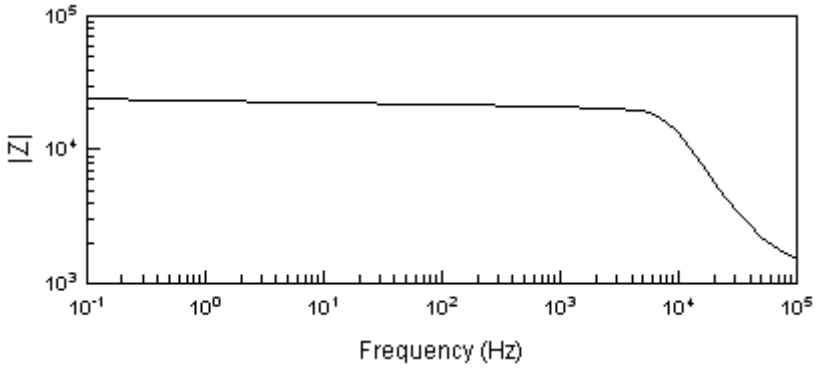

Figure 4-25B Bode diagram for set 6 at day 37

- Bare steel samples with sealant only

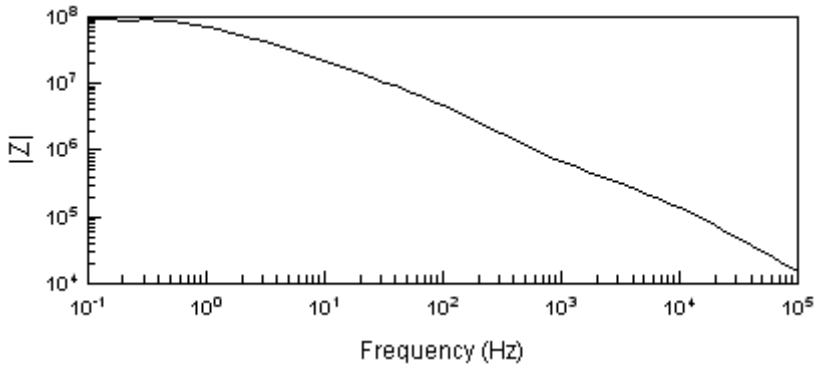

Figure 4-26A Bode diagram for bare steel samples at day 1

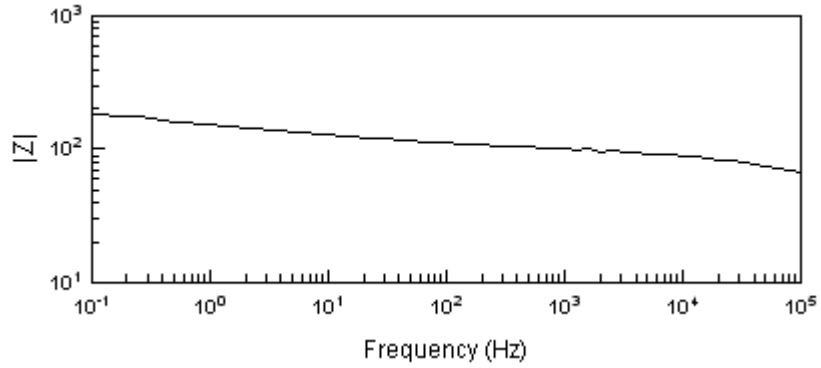

Figure 4-26B Bode diagram for bare steel samples at day 37

As mentioned in the literature review, the EIs technique is usually used to investigate the performance of coating systems in terms of the quality of the materials used to make the coating and the corrosion process under the coating. Based on Mansfield approach, a good coating tends to show one time constant (the semi-circuit appears in Nyquist Plot). Such time constant represents the quality of the coating. In general, two important values are obtained from such plot, Pore Resistance (Rp which is directly related to the ionic conductivity of the coating) and the coating capacitance (Cp which represents the water uptake in the coating).

From the EIS data and figures above, the resistances of all coatings dropped suddenly after 24 hours indicating that the water and oxygen reached the surface and a

corrosion process was started. Such findings indicate that the coatings systems have not shown the required protection to the steel.

Table 4-2 AC Impedance pore resistance data for set 3, 5, 6 and bare steel

Day	**Set 3**	**Set 6**	**Set 7**	**Bare steel**
1	1.13E+08	8.06E+07	9.87E+07	4.98E+07
2	2.23E+05	2.96E+05	1.65E+05	1.36E+05
4	2.01E+04	7.98E+03	5.50E+03	2.60E+02
5	6.10E+04	5.67E+04	5.65E+04	1.58E+02
9	6.03E+04	6.33E+04	4.58E+04	1.20E+02
10	5.18E+04	5.98E+04	2.95E+04	9.93E+01
11	3.23E+04	4.03E+04	2.05E+04	3.72E+02
12	1.65E+04	4.06E+04	2.70E+04	1.31E+04
16	2.60E+04	3.62E+04	2.58E+04	9.61E+02
37	2.60E+03	4.14E+04	2.52E+04	4.05E+01

The figure below plot the pore resistance for each set along with bare steel samples against number of exposure days.

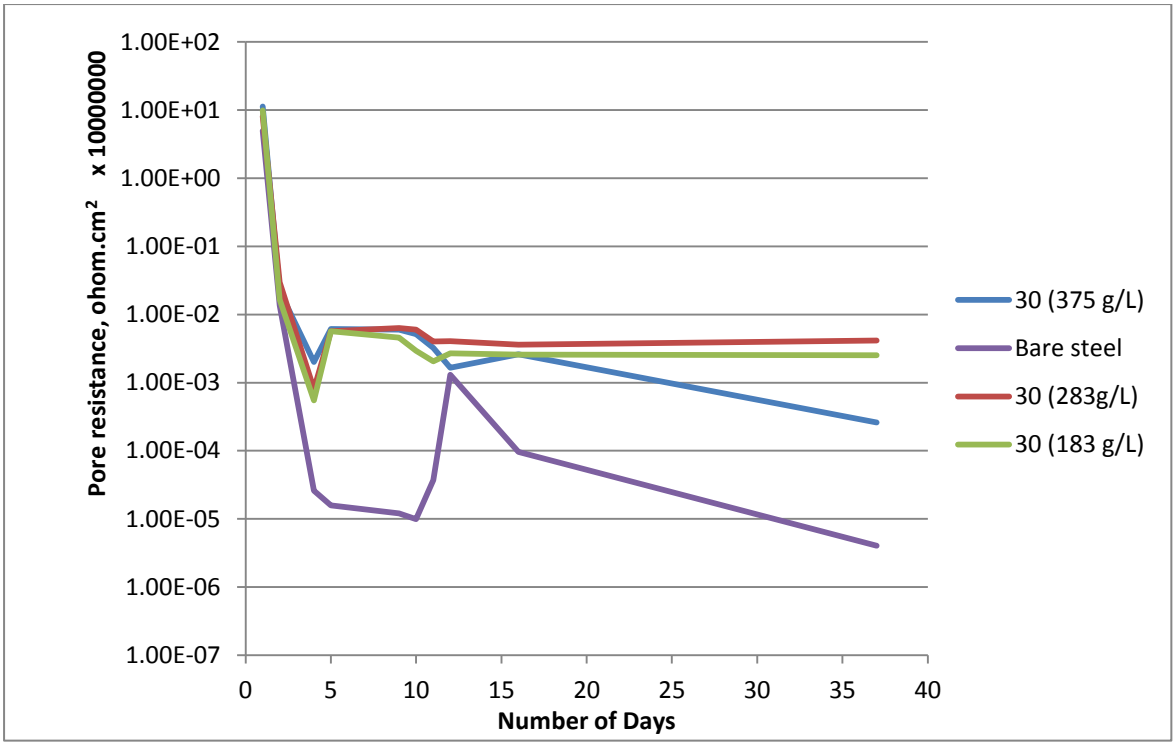

Figure 4-27 AC Impedance Data for sets 3, 5, 6 and bare steel

The figure above shows that all sets (3, 5 and 6) have showed higher pore resistance comparing to bare steel. The start value of the pore resistance for these sets was almost double of even triple times the pore resistance in case of bare steel. This is a good indication that these sets at 30 ml/ min flowrate added some improvements to the target substrates and acts as barrier better than bare steel samples. On the other hand, sets 2 and 4 which were produced at 50 ml/ min showed different behavior comparing to 30 ml/min as shown in the table and figure below.

Table 4-3 AC Impedance data for set 2, 4 and bare steel

Day	Set 2	Set 4	Bare steel
1	2.41E+07	4.64E+07	4.98E+07
2	2.42E+05	5.57E+05	1.36E+05
4	2.72E+04	2.83E+03	2.60E+02
5	5.18E+04	4.77E+04	1.58E+02
9	5.23E+04	2.20E+04	1.20E+02
10	5.08E+04	1.33E+04	9.93E+01
11	3.05E+04	3.03E+04	3.72E+02
12	1.95E+04	2.14E+04	1.31E+04
16	2.34E+04	1.19E+04	9.61E+02
37	9.43E+03	6.80E+03	4.05E+01

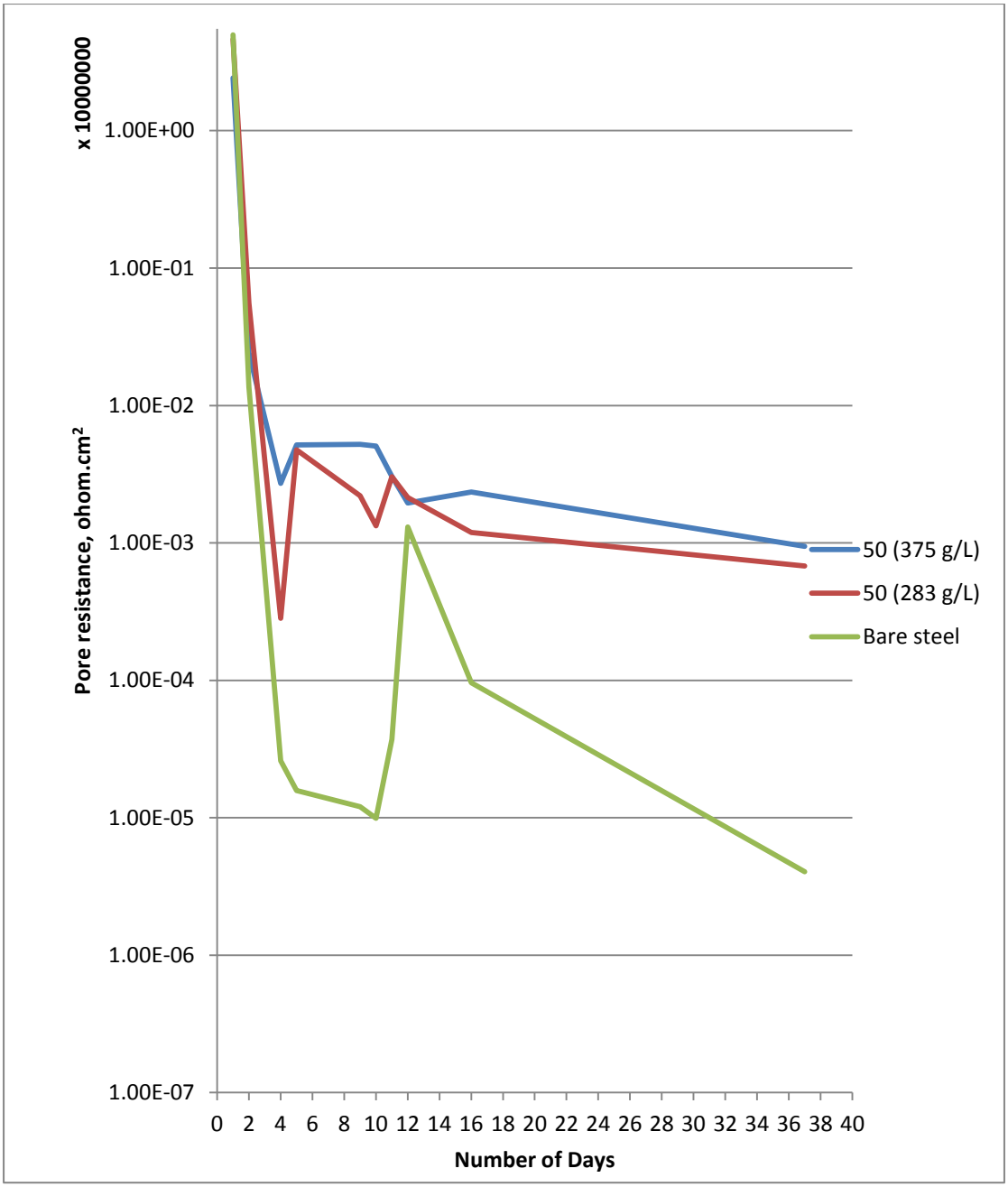

Figure 4-28 AC Impedance Data for sets 2, 4 and bare steel

4.4 XRD and SEM Analysis

XRD and SEM analysis were conducted on several samples and the main purpose of this SEM, EDS and XRD study is to characterize aluminum oxide top coating layer on the selected carbon steel substrates. SEM technique was utilized for plan view and cross section. The plan view analysis was conducted just to show the morphology of each substrate and cross section was conducted in order to obtain information about layers of the coating and thickness of top layer. XRD technique was used to study the phase change in the coating and therefore, effect of flowrate and concentration on phase change. The samples which were included in this kind of characterization were mentioned in table 3-8 chapter 3. The results of XRD and SEM techniques can be summarized as follows:

The samples were placed on the ESEM sample holder (stub) using a double-sided carbon tape and the ESEM was operated at 15kV, 0.15-0.90 torr water vapor pressure with 6-10.4mm working distance. Topographical backscattered and secondary electron images were acquired at magnifications ranging from 250 to 30,000 times. The ESEM and EDX findings for the plan view and cross sectional samples revealed that the outermost layer consists of Al_2O_3 as shown in figure 4-29.

Set 2

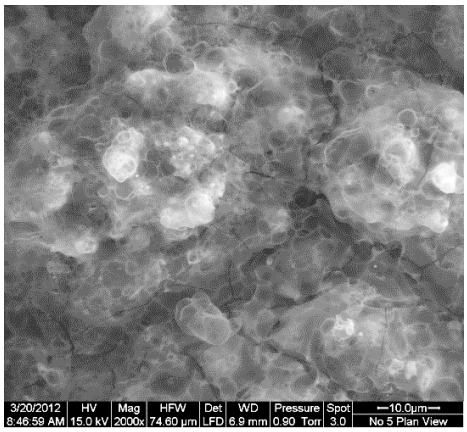

Set 3

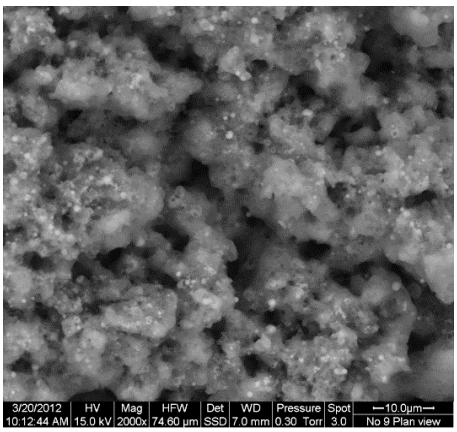

Set 5

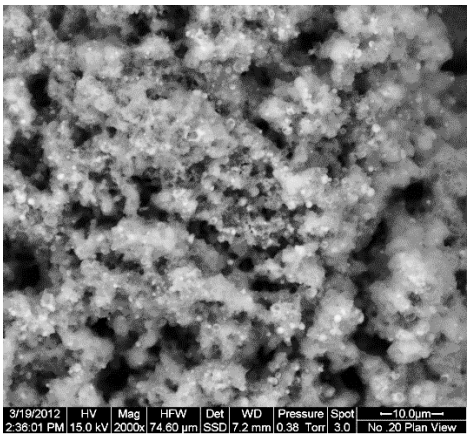

set 6

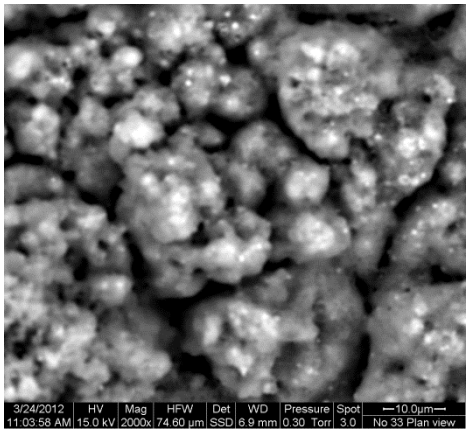

Figure 4-29 SEM Analysis

The XRD data showed the formation of γ-aluminum oxide layer as shown in figure 4-30 and no significant differences in the texture of the formed γ-aluminum oxide layers were observed.

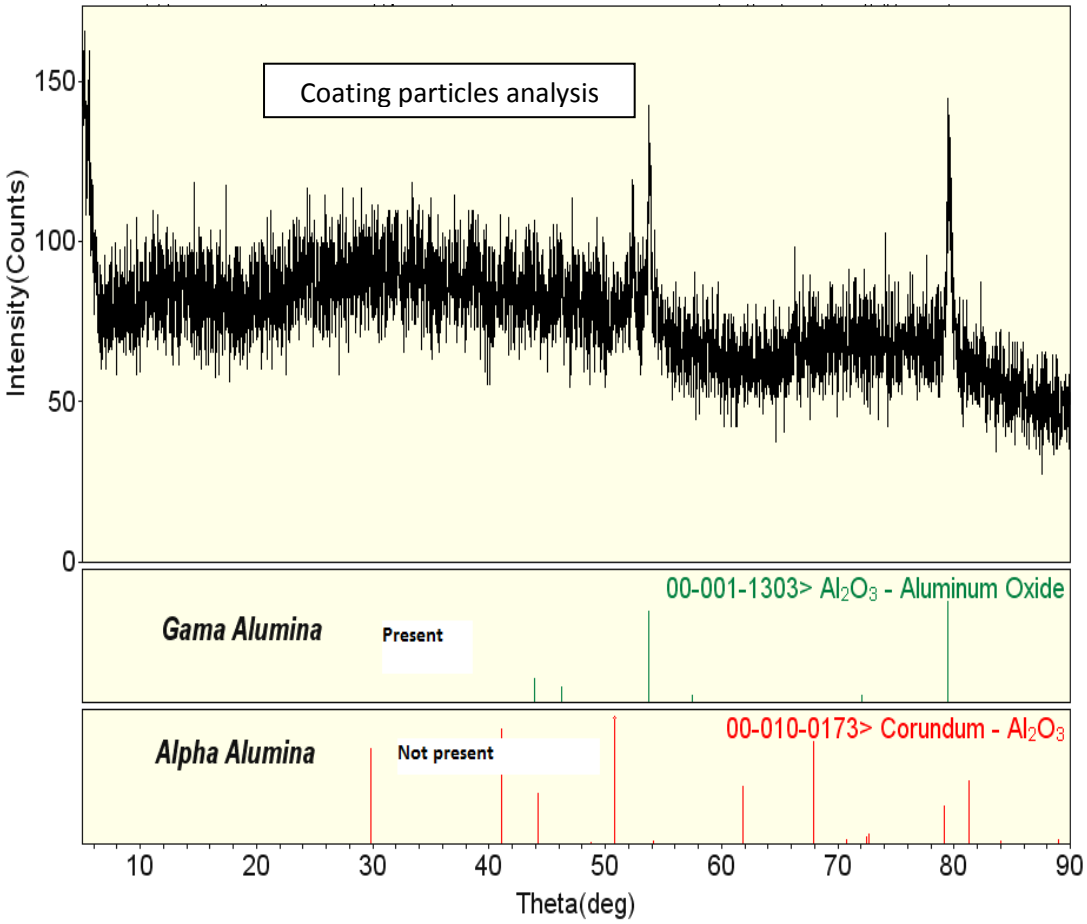

Figure 4-30 XRD Analysis for aluminum oxide layer

The ESEM image using linescans from the cross-sectional samples and the scale thickness measurements showed that the thickness of outermost layer "aluminum oxide" ranges from 25.83 to 35.36 microns as shown in the figures below for each set of samples.

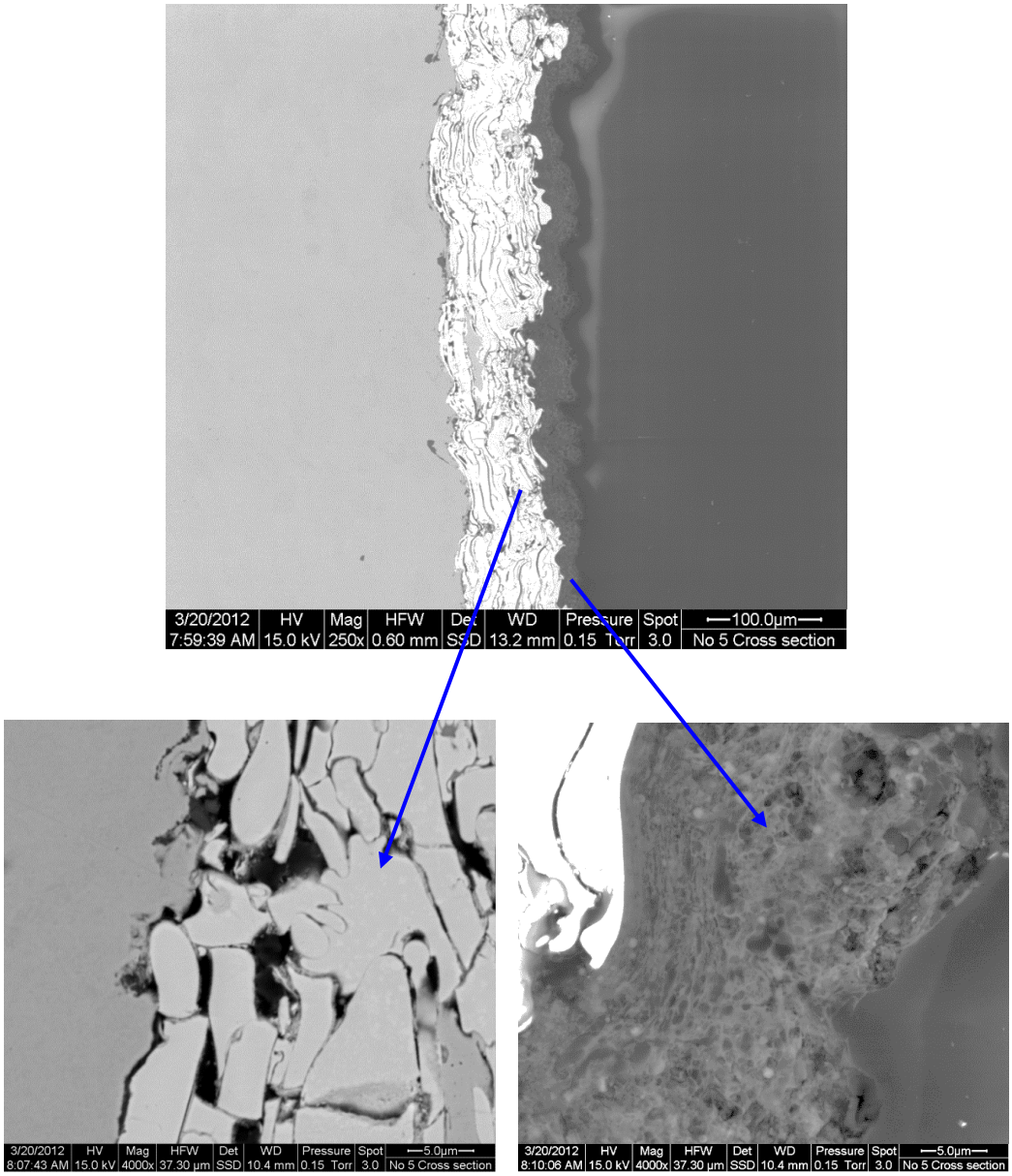

Figure 4-31A Backscattered electrons images for set 2

This figure (4-31A) shows coating layers, the bond coat and aluminum oxide coating where some voids are observed in the bond coat and aluminum oxide coating layer is more dense coating in set 2.

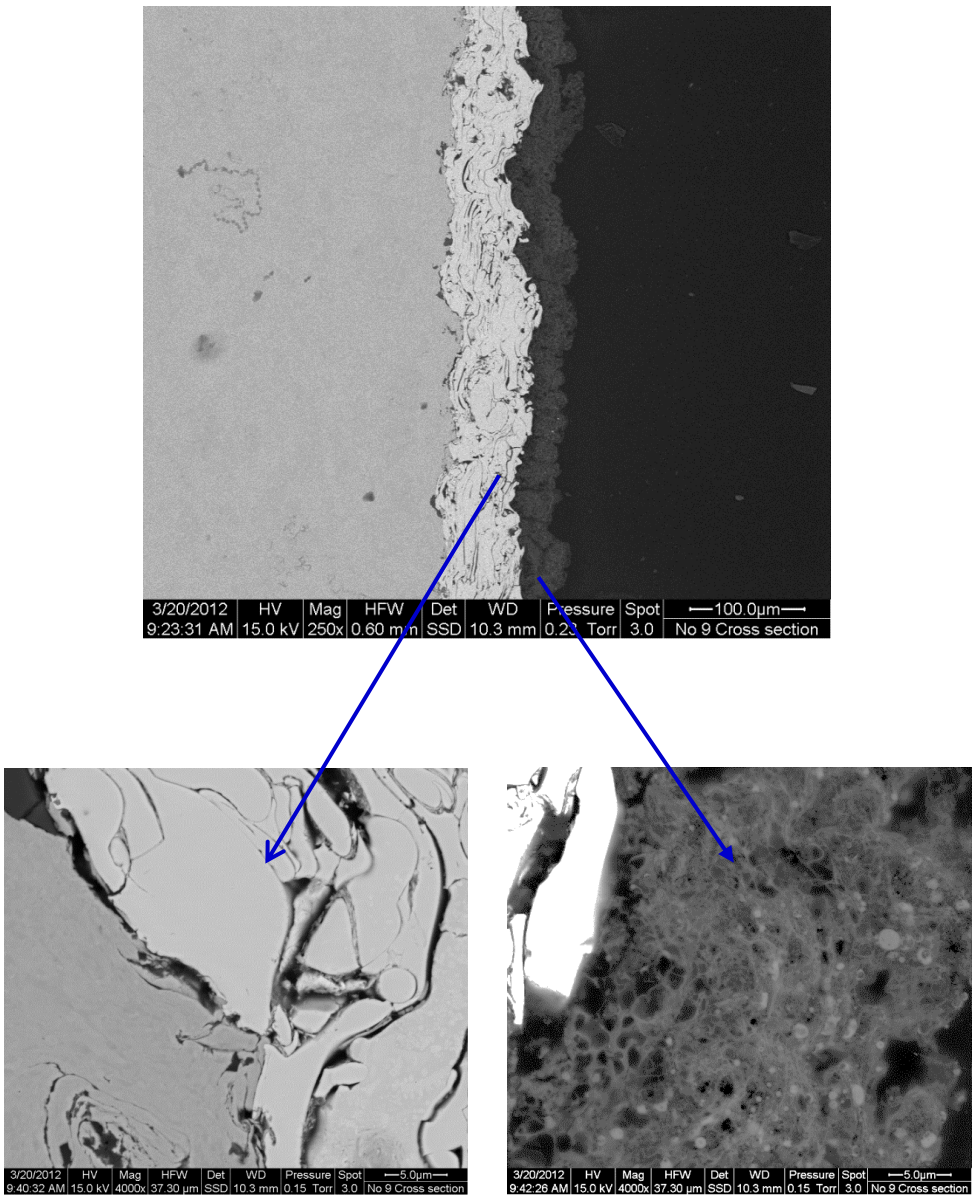

Bond coat layer Aluminum oxide layer

Figure 4-31B Backscattered electrons images for set 3

This figure (4-31B) shows backscattered images for both coating layers, the bond coat and aluminum oxide coating where some voids are observed in the bond coat and aluminum oxide coating layer has more porosity comparing to set 2. This means that, higher flowrate than 30 ml/min will decrease the porosity in the top coating layer.

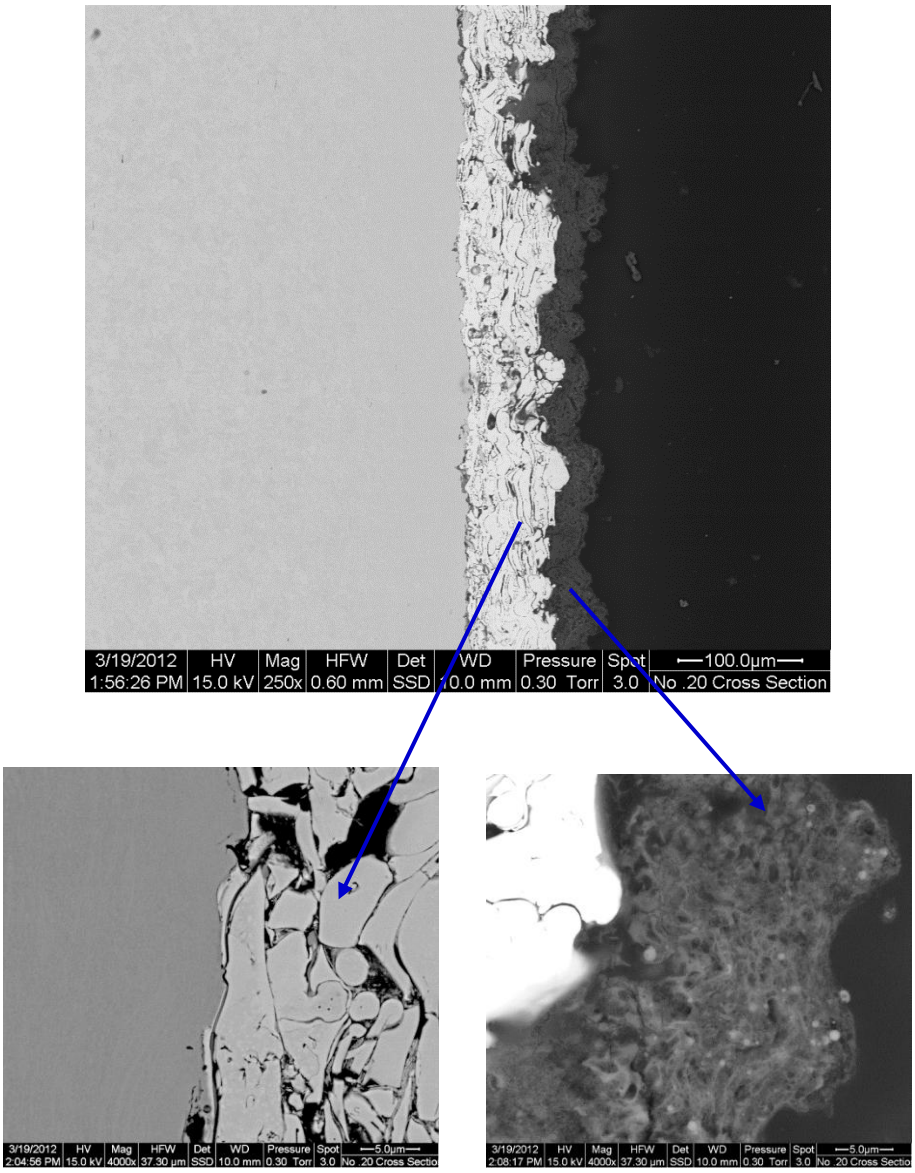

Bond coat layer Aluminum oxide layer

Figure 4-31C Backscattered electrons images for set 5

This figure (4-31C) shows backscattered images for both coating layers, the bond coat and aluminum oxide coating. It is clear from the figure above that some voids are observed in the bond coat but aluminum oxide coating layer has higher porosity comparing to set 2.

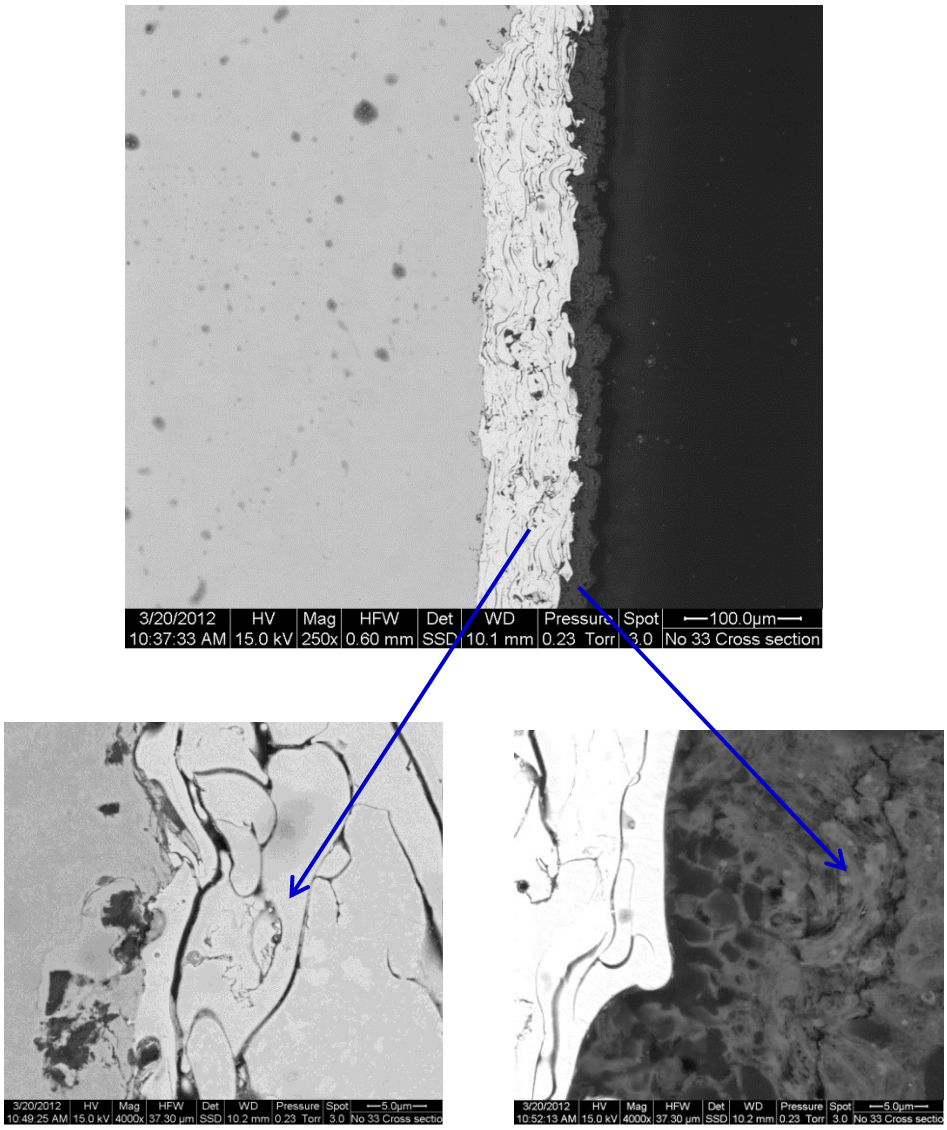

Figure 4-31D Backscattered electrons images for set 6

Both SEM/EDX analyses and XRD patterns showed that the top coating layer which is aluminum oxide coating comprises mainly agglomerated fine particles of γ-aluminum oxide and there are no significant differences in the formed layers on all the tested samples. This may suggest that changing the coating conditions such as flow rate and concentration of aluminum nitrite did not affect the coating morphology or texture. Therefore, lowering the concentration of the aluminum nitrate from 1125 g to

550 g will have same behavior also; it will reduce the total cost of aluminum nitrate material by around 40 - 50%.

The coating thickness of the outer coating layer varies from approximately 25.83 to 35.36 microns and appeared to be higher in the case of set number 3. The table below summarizes thickness measurements for each sample as follows:

Table 4-4 Coating thickness measured by SEM

Set number	**Coating Conditions**		
	Flow rate ml/min	**Concentration g/ liter**	**Coating Thickness (microns)**
2	50	375	25.97
3	30	375	35.36
5	30	283	27.48
6	30	183	25.85

CHAPTER 5

5 CONCLUSION AND RECOMMENDATIONS

5.1 Conclusion

Aluminum oxide nano-structured coating was produced as thin films at three different concentrations of Aluminum nitrate nona-hydrate and three different flowrates of the solution by using solution plasma spray feeder. This coating thin film was tested in the aqueous environment and characterized by using SEM and XRD techniques. The following items were concluded based on the findings and results from the experimental work in this master thesis:

- Solution Plasma Spray (SPS) technique can be used as feedstock along with thermal plasma spray system as energy source to produce aluminum oxide nano-structured coatings.
- Therefore, SPS can be introduced as a new technique that can be utilized to produce aluminum oxide coating from aluminum nitrate nona-hydrate solution.
- Aluminum oxide coating layer at same conditions and parameters mentioned in this master thesis cannot be considered as protective coating against corrosion in the aqueous environment due to the presence of porosity.
- Polyurethane sealant can enhance the pore resistance of the coating system to some extent by minimizing the porosity of the aluminum oxide coating. However, other sealant can be evaluated to identify better sealant to be part of the coating system.

- All samples that were sprayed using high solution flowrate (> 50 ml/min) showed coating delamination with many cracks developed on the surface of the coating layer. Therefore, no coating was achieved at higher concentrations.
- Low flowrates (< 50 ml/min) of the aluminum nitrate solution showed better coating layer with uniform coating and no cracks were observed.
- Higher concentration of the aluminum nitrate solution with low flowrate has showed higher thickness than other parameters.
- Lower concentrations runs of sprayed aluminum nitrate solution showed same behavior and phase (γ-alumina) as well as higher concentrations of same solution.
- Bond coat layer (CoCrAlY) acts as adhesion promotion and oxidation resistance layer.
- Overall performance for all coating systems has not showed the expected corrosion protection, however, slight improvements have been observed.

5.2 Recommendations

After investigating the generated data out of this research study, the following recommendations can be considered in the future work:

- It is clearly spotted out that the mechanical properties of the prepared coating need to be improved. Accordingly, incorporation of nanofillers such as nano-clay can be a value adding component to enhance the mechanical properties. These fillers can be added to the solution in the SPS.
- Considering an alternative sealant such as Epoxy resin can improve the barrier properties of the coating system.

References

1. Long-term atmospheric corrosion of mild steel; D. de la Fuente, I. Díaz, J. Simancas, B. Chico, M. Morcillo, 2010

2. Corrosion-resistant metallic coatings for applications in highly aggressive environments; N. Priyanthaa, P. Jayaweeraa, A. Sanjurjoa, K. Laua, F. Lua, K. Kristb, 2003

3. Investigation of the corrosion behavior of carbon steel coated with fluoropolymer thin films Amel Delimi a,b,c, Elisabeth Galopin a,b, Yannick Coffinier a,b, Marcin Pisarek d, Rabah Boukherroub a,b, Brahim Talhi c, Sabine Szunerits, 2011

4. Corrosion-resistant metallic coatings on low carbon steel; P. Jayaweera, D.M. Lowe, A. Sanjurjo, K.H. Lau, L. Jiang, 1996

5. Investigation into the effects of metallic coating thickness on the corrosion properties of Zn–Al alloy galvanising coatings, David J. Penney, James H. Sullivan, David A. Worsley, 2007

6. Characterization of flame-sprayed and plasma-sprayed pure metallic and alloyed coatings; I.Iordanova ", K.S. Forcey b, B. Gergov a, V. Bojinov, 1994

7. A method of Evaluating Thermal Spray Process Performance. R. Molz, D. Hawley.

8. Effect of bond coat nature and thickness on mechanical characteristic and contact damage of zirconia-based thermal barrier coatings, Jae-Young Kwon a, Jae-Hyun Lee a, Yeon-Gil Jung a,□, Ungyu Paik, 2006

9. Microstructural evolution of CoCrAlY bond coat on Ni-based superalloy DZ 125 at 1050 °C, Tianquan Liang a,b,c, Hongbo Guo a,c,□, Hui Peng a,c, Shengkai Gong,

10. Low thermal conductivity thermal barrier coating deposited by the solution plasma spray process, Xinqing Ma a,, Fang Wu , Jeff Roth , Maurice Gell , Eric H. Jordan, 2006.

11. The corrosion behaviour of a plasma spraying Al_2O_3, ceramic coating in dilute HCl solution

12. Nanocrystalline gamma alumina coatings by inverted cylindrical magnetron sputtering, Atul Khanna 1, Deepak G. Bhat, 2005.

13. Evans, U.R., Metallic corrosion, passivity and protection 1946, London: E. Arnold and Co.

14. Shreir, L.L., R.A. Jarman, and G.T. Burstein, Corrosion: MetaVEnvironment Reactions. Third ed. Vol. 1. 1994, Oxford: Butterworth-Heinemann.

15. Jones, D.A., Principles and Prevention of Corrosion. Second ed. 1996, New Jersey, USA: Prentice-Hall Inc.

16. Evans, U.R., The corrosion and oxidation of metals 1976, London Edward Arnold.

17. Butler, G. and B.C.K. Ison, Corrosion and Its Prevention in Waters. Second ed. 1978, New York. 62-63.

18. Scully, J.C., The Fundamentals of Corrosion. Third ed. 1990, Oxford, UK. 100-101.

19. Kuznetsov, Y.I., Organic inhibitors of corrosion of metals. 1996, London, New York: Plenum Press.

20. Turgoose, S. and M. Pech-Canul, The Electrochemical Impedance Response Of Film-Covered Mild Steel in Neutral Aerated Solution. Corrosion Science, 1993. **35**: p. 1445-1454.

21. Olivares-Xometl, O., et al., Synthesis and corrosion inhibition of amino acids alkylamides for mild steel in acidic environment. Materials Chemistry and Physics, 2008. **110**: p. 344–351.

22. Plasma resistant aluminum oxide coatings for semiconductor processing apparatus by atmospheric aerosol spray method; Hoomi Choi, Kwangsu Kim, Heesung Choi, Sangwoo Kang, Juyoung Yun, Yonghyeon Shin, Taesung Kim, 2010

23. Aluminum oxide barrier coating on polyethersulfone substrate by atomic layer deposition for barrier property enhancement; Hyun Gi Kim, Sung Soo Kim, 2010

24. High hardness alumina coatings prepared by low power plasma spraying Yang Gao, Xiaolei Xu, Zhijun Yan, Gang Xin, 2001

25. Microstructure and tribological behavior of suspension plasma sprayed Al_2O_3 and Al2O3–YSZ composite coatings O. Tingaud, P. Bertrand, G. Bertrand; 2010

26. Evaluation of Adhesion/Cohesion of Plasma Sprayed Ceramic Coatings by Scratch Testing. J. Zhang, H. Chen, S. W. Lee.

27. Sulzer Metco LTD, www.sulzermetco.com, 2007. 5

28. Inframat Corporation; http://www.inframat.com/sps.htm, 2010

29. Wicks, Z.W., et al., Organic Coating: Science and Technology Third ed. 2007, Hoboken, N.J, USA: John Wiley and Sons.

30. Shreir, L.L., G.T. Burstein, and R.A. Jarman, Corrosion: Corrosion Control. Vol. 2. 1994, Oxford: Butterworth-Heinemann.

31. Macdonald, D.D. and M.C. McKubre, Electrochemical Impedance Techniques in Corrosion Science. American Society for Testing and Materials, 1981: p. 110-149.

32. Cottis, R. and S. Turgoose, Electrochemical Impedance and Noise, ed. B.C. Syrett. 1999, Houston, USA: NACE International.

33. Macdonald, D.D., Transient Techniques in Electrochemistry. 1977, New York, USA: Plenum Press.

34. Mansfeld, F., S.L. Jeanjaquet, and M.W. Kendig, An Electrochemical Impedance Spectroscopy Study of Reactions at the Metal/Coating Interface. Corrosion Science, 1986. **20**: p. 735-74.

35. Bonora, P.L., F. Deflorian, and L. Fedrizzi, Electrochemical Impedance Spectroscopy As a Tool For Investigating Underpaint Corrosion. Electrochemica Acta., 1996. **41**: p. 1073-1082.

36. Mansfeld, F., Electrochemical Impedance Spectroscopy (EIS) As a New Tool For Investigating Methods Of Corrosion Protection. Electrochemica Acta., 1990. **35**: p. 1533-1544,.

37. Tang, N., W.J.V. Ooij, and G. Corecki, Comparative EIS Study of Pretreatment Performance in Coated Metals. Progress in Organic Coating, 1997. **30**: p. 255-263.

38. Ranjbar, Z., et al., EIS Investigation of Cataphoretically Electrodeposited Epoxy Coatings Having Different EEWs. Progress in Organic Coating, 2004. **51**: p. 87-90.

39. Scantlebury, J.D. and K. Galic, The application of AC impedance to study the performance of lacquered aluminium specimens in acetic acid solution. Progress in Organic Coating, 1997. **31**: p. 201-207.

40. Mansfeld, F., et al., Evaluation Of Corrosion Protection by Polymer Coatings Using Electrochemical Impedance Spectroscopy and Noise Analysis. Electrochemica Acta., 1998. **43**: p. 2933-2945.

41. Mansfeld, F., A.L. Rudd, and C.B. Breslin, The corrosion protection afforded by rare earth conversion coatings applied to magnesium. Corrosion Science, 2000. **42**: p. 275-288.

42. Ciubotariu, A.C., et al., Electrochemical impedance spectroscopy and corrosion behaviour of Al2O3–Ni nano composite coatings. Electrochemica Acta., 2008. **53**: p. 4557–4563.

43. Scantlebury, J.D. and J. Colreavy, Electrochemical impedance spectroscopy to monitor the influence of surface preparation on the corrosion characteristics of

mild steel MAG welds. Journal of Materials Processing Technology, 1995. **55**: p. 206-212.

44. Bragg, W., An introduction to crystal analysis. 1928, London.

45. Cullity, B.D., Element of X-Ray Diffraction. Third ed. 1967, Reading, Massachusetts, London: Addison-Wesley Publishung Company.

46. Lipson, H. and H. Steeple, Interpretation of X-ray power diffraction patterns. 1970, London: Macmillan.

47. Klug, H.P. and L.E. Alexander, X-Ray diffraction Procedures. Second ed. 1974, New York ; London Wiley-Interscience.

48. Goodhew, P.J., J. Humphreys, and R. Beanland, Electron Microscopy and Analysis. Third ed. 2001, London, UK: Taylor & Francis. 122-213.

49. Goldstein, J.I., et al., Scanning Electron Microscopy and X-Ray Microanalysis 1981, New York ; London Plenum.

50. Hall, J.L., Electron Microscopy and Cytochemistry of Plant cells. 1978, Amsterdam ; Oxford Elsevier/North-Holland Biomedical Press.

NOMENCLATURE

SPS: Solution Plasma Spray

EIS: Electrochemical Impedance Spectroscopy

SEM: Scanning Electorn Microscope.

EDS: Energy-dispersive X-ray spectroscopy

CP: Cathodic Protection

PVD: Physical Vapor Deposition

CVD: Chemical Vapor Deposition

AC: Alternative Current

C_{dl}: Double layer capacitance

C_c: Coating Capacitance

R_p: Polarization Resistance

I_{corr}: Corrosion Current

β_a and β_b: Tafel Coefficient

VITA

Name	Bander Faraj Al-Daajani
Religion	Islam
Nationality	Saudi
Place and Date of birth	Sudair, Saudi Arabia, June 1976
Address	Saudi Aramco, Dhahran 31311 Saudi Arabia
Email Address	daajan2005@yahoo.com
Contact Information	Office: 8768166 Mobile: 0506424057
Education	Bachelor of science in chemical engineering from King Saud University in June 2000
Education	Master of science in chemical engineering from King Fahd University of Petroleum and Minerals in May 2012